RESEARCH TRIANGLE INSTITUTE

July 1988

Phase I — Final Report

Catalytic Dehydration of Methanol

Prepared by

Don R. van der Vaart
Research Triangle Institute
Research Triangle Park, NC 27709

Prepared for

Robert M. Heavenrich, Project Officer
U.S. Environmental Protection Agency
Ann Arbor, MI 48105

EPA Contract No. 68-03-3527
RTI Project No. 4002

Phase I — Final Report

Catalytic Dehydration of Methanol

Prepared by

Don R. van der Vaart
Research Triangle Institute
Research Triangle Park, NC 27709

Prepared for

Robert M. Heavenrich, Project Officer
U.S. Environmental Protection Agency
Ann Arbor, MI 48105

EPA Contract No. 68-03-3527
RTI Project No. 4002

July 1988

CONTENTS

FIGURES

TABLES

ABSTRACT

The results of Phase I of EPA Contract No. 68-03-3527 are presented. It is apparent that several commercially available catalysts are suitable for the methanol dehydration reaction forming dimethyl ether. Problems in developing a prototype dehydration reactor suitable for mounting under the hood of an automobile are presented. In particular, the exothermicity of the methanol dehydration reaction can result in a runaway temperature excursion within the reactor. This can lead to the loss of product selectivity by the formation of higher hydrocarbons with the concomitant formation of coke, which can lead to catalyst deactivation. Although more sophisticated reactor designs can be used to minimize the likelihood of these excursions, the reaction system is quite sensitive to slight changes in operating conditions.

It is proposed, in Phase II, to study the kinetic rate of both the methanol dehyrdation reaction for a limited group of dehydration catalysts as well as the methanol dissociation reaction over available dissociation catalysts. With this information, a relatively simple theoretical analysis is feasible by which a dehydration/dissociation catalyst mixture reactor could be designed. The dissociation reaction pathway would be provided only as a heat sink to prevent reactor runaway.

Finally, it is shown that the process energetics for such a reactor would require the condensation of the product stream in order to allow operation without a significant amount of external power requirements. A simple phase equilibrium analysis is presented which shows that the condensed product stream is suitable for cold-starting an internal combustion in a mechanism completely analogous to winterized gasoline.

SECTION 1
INTRODUCTION

Methanol can be used as a motor fuel with considerable environmental advantages over gasoline. Its use in various mixtures with gasoline is currently being tested by both the Ford Motor Company and ARCO. Using 100% methanol rather than blending it with a winterized gasoline, while representing a truly alternative fuel with excellent emission characteristics, does present certain problems. In particular, the high heat of vaporization of methanol (more than seven times that of gasoline on a per Btu heating value basis) combined with the higher fuel to air ratio required for combustion (approximately twice that of gasoline) causes severe cold starting problems. To this end the U.S. Environmental Protection Agency (EPA) has suggested that under cold starting conditions an amount of methanol fuel could be catalytically dehydrated to form dimethyl ether (DME) via the following reaction:

$$2CH_3OH \rightleftharpoons CH_3OCH_3 + H_2O \quad . \qquad (1)$$

DME exhibits favorable combustion characteristics and is satisfactorily volatile.

The catalytic dehydration of methanol is a well-studied reaction. It forms the first step in Mobil's patented Methanol to Gasoline (MTG) process as well as being an integral part of other chemical production processes. From the literature relative to reaction (1) two conclusions can be drawn:

- Catalytic dehydration of methanol vapor to dimethyl ether is an acid catalyzed reaction. Lewis acid sites and almost certainly fairly weak Lewis base sites are necessary on the surface of any successful catalyst. Strong Bronsted acidity promotes the further reaction of DME to olefins and paraffins.
- While most research on this reaction has focused on various conventional zeolites, other catalysts have been shown to be successful. These include metal salts, alumina, silica alumina, alumino phosphate molecular sieves, ion exchange resins, and mixed metal oxides.

As an example of the work published in the development of Mobil's MTG process, Figure 1 shows the effect of the space time (liquid hourly space velocity $(LHSV)^{-1}$) (defined as the volumetric flowrate of liquid methanol divided by

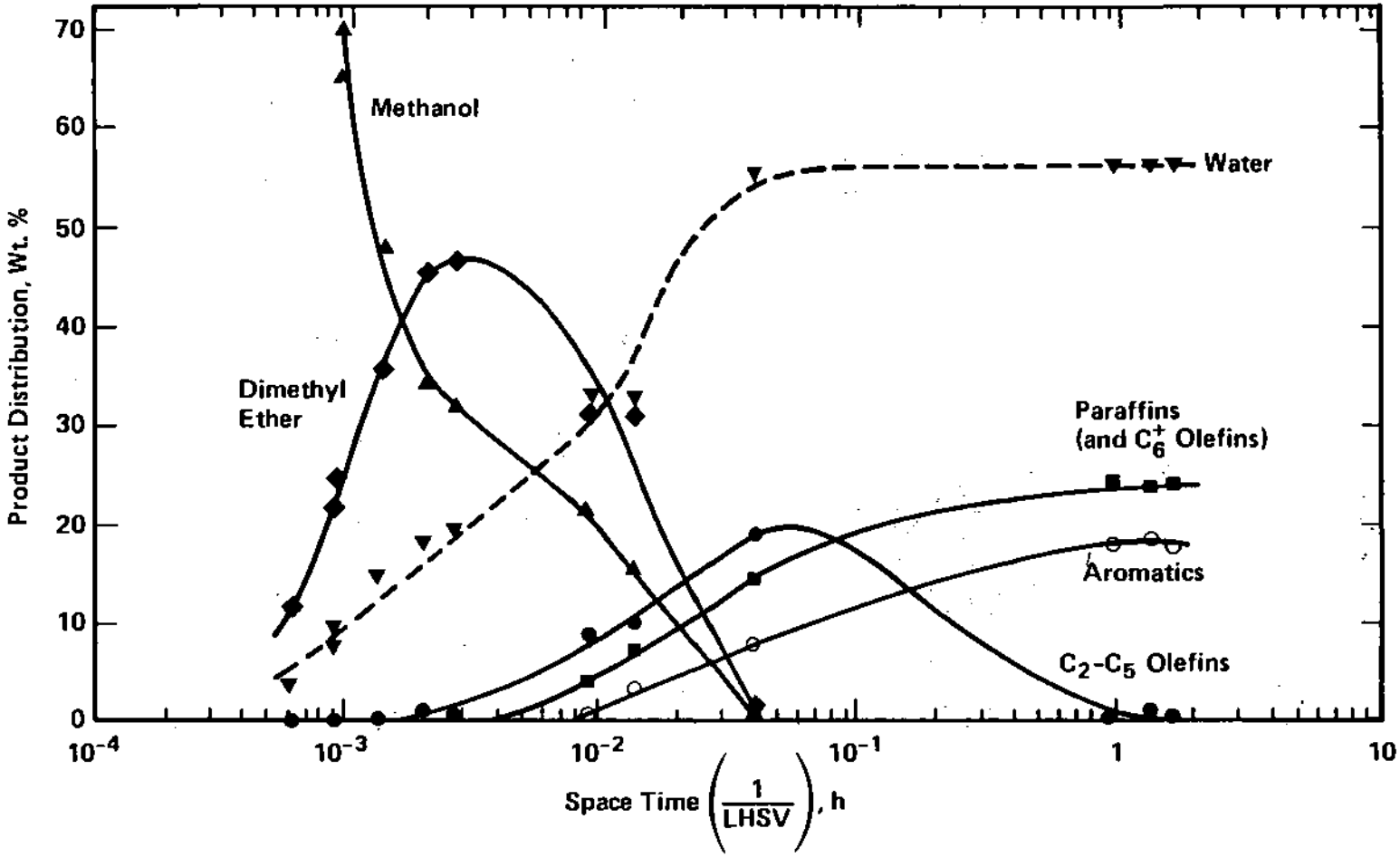

Figure 1. The effect of space time on product distribution (T = 371 °C, P = 1 atm) [1].

the volume of catalyst) on product distribution over a zeolite catalyst. [1] Figure 1 also illustrates the series reactions that can occur in this system. That is

$$A \overset{\rightarrow}{\leftarrow} B + C \qquad (2)$$

where A is methanol, B is dimethyl ether, and C constitutes a variety of hydrocarbon products which make up the gasoline fraction produced by the MTG process. Obviously, it is this latter product fraction which Mobil attempts to maximize. The formation of these hydrocarbons (aromatics, olefins, and some paraffins) has associated with it, however, the formation of carbonaceous deposits on the catalysts (i.e., coke). This byproduct has the effect of deactivating the catalyst over time, necessitating its regeneration. The goal of the present work is not to produce gasoline *in situ* but rather to provide a volatile product suitable for starting the vehicle in cold weather. Dimethyl ether formed as an intermediate in reaction (2) meets this objective without the associated deactivation of the catalyst. In fact, Mobil has remarked [2] that their first stage unit, which produces DME at equilibrium conversion, has yet to experience catalyst deactivation at their plant in New Zealand, while their second stage DME-to-gasoline reactor requires continuous regeneration. The work presented herein attempts to produce a methanol/DME mixture suitable for starting an engine.

Previous work [3] indicates that this mixture should be roughly 10 to 15 percent (by volume) DME in methanol. In terms of Figure 1, then, a reactor should operate with a space time (1/LHSV) of roughly 10^{-3} hr under the conditions studied in that work, (i.e., 371° C, 1 atm).

SECTION 2
CANDIDATE CATALYSTS

A discussion of the catalytic chemistry involved in the dehydration of methanol to dimethyl ether is beyond the scope of this report. Several investigations of this reaction by various researchers [1,4,5] have been reported. In the particular application of methanol dehydration to facilitating the cold starting of an automobile engine, three criteria that the optimal catalyst should meet are:

- the catalyst must be sufficiently active to produce a product stream capable of satisfying the cold starting requirements of an engine (roughly 15% DME in methanol).
- the catalyst must be stable under temperature excursions.
- the catalyst must be economical when normalized by its expected lifetime. Deactivation will likely occur due either to coking reactions caused by further dehydration of DME to unsaturated hydrocarbons (reaction (2)) or to high temperature sintering.

A list of various catalyst families suitable for the dehydration reaction along with some of their advantages and disadvantages is presented in Table 1.

Upon award of this contract, a number of commercial catalyst vendors were contacted to obtain catalysts suitable for the methanol dehydration reaction. An example of the request is given in Appendix A. Of the catalyst families listed in Table 1, only four were represented by samples received in response to this solicitation. These are presented in Table 2 categorized by family. A brief description of these catalysts, including the limited information provided by each vendor, is presented below.

Alumina

Aluminum oxide (Al_2O_3) exhibits significant acid properties suitable for methanol dehydration reaction. These acid properties can be varied somewhat by the calcining procedure used in their manufacturing so that a large variety of aluminas exist. Harshaw/Filtrol provided a number of alumina catalysts as listed in Table 2. A summary of the composition of each of these catalysts is presented in Table 3. The properties of the United Catalyst alumina catalysts are presented in Table 4. Note that the surface areas do vary somewhat.

Table 1. Advantages and Disadvantages of Candidate Catalyst Families

Catalyst	Advantages	Disadvantages
Zeolites		
aluminosilicates	Much research has been done on this catalyst; methanol dehydration is fairly well understood	Possible selectivity problems since DME readily react further on these catalysts
aluminophosphates	Probably has the right mix of acid-base site strengths	Relatively new materials; methanol dehydration has not been well studied
Silica-aluminas	Well-studied catalysts for this reaction	High density of very strong acid sites may lead to low selectivity and/or coking
	Bronsted/Lewis acid site ratio is controllable by calcining conditions	
	Low cost catalyst	
Aluminas	Acid strength distribution is controllable by calcining temperature	Selectivity may be poor; alumina is very active for olefin formation from alcohol dehydration
	Bronsted/Lewis acid/base character is controllable by dehydroxylation	Small amounts of impurities can affect the acid site strength and thus the activity/selectivity
Metal salts		
phosphates	May have surface acidity comparable to alumina	Selectivity may be poor due to strength of acid sites
sulfates	Bronsted/Lewis acid-base sites are controllable by calcination	Inherently strong acid sites may lead to coking

(continued)

Table 1 (continued)

Catalyst	Advantages	Disadvantages
Ion exchange resins	High activity at low temperatures	Poor mass transfer in some resins due to small pore sizes
	Acidity is controllable by synthesis conditions	Deactivation may occur if temperature excursions above ~150° C occur
Mixed metal oxides	Acid site strength controllable by synthesis conditions	Selectivity may be poor since some mixed oxides also promote dehydrogenation and olefin formation.

Table 2. Catalyst Samples Received and Tested

Aluminas		
	Harshaw	AL-5207 AL-5307 AL-5407 AL-3945 AL-3996R
	United	CS 331-1 CS 331-4
Zeolites		
	Union Carbide	LZ-20 LZ-Y-72 LZ-M8
	United	Z6-06-02
	Mobil	MCG-7 MCG-8
Metal oxides		
	Zeochem	Z6-06-02, B6980
	Harshaw	ZR-0304T TI-0720
	United	T-312 T-314 T-317 T-1502A T-1502B 7913-S, K-306
Ion Exchange Resins		
	Rohm & Haas	XE-386 6-928 Not tested 6-9852

Table 3. Harshaw/Filtrol Alumina Catalysts

Catalysts	Surface Area (m^2/g)	Composition (wt%) w/Balance Al_2O_3 Fe_2O_3	SiO_2	Na_2O
AL-5207	200	0.1	0.2	0.08
AL-5307	200	0.1	0.2	0.08
AL-5407	190	0.1	0.2	0.08
AL-3945	250	< 0.01	< 0.01	< 0.01
AL-3996R	200	0.07	0.01	0.06

Table 4. United Catalyst Alumina Catalysts

Catalysts	Surface Area (m^2/g)	Composition (wt%) w/Balance Al_2O_3 Fe_2O_3	Na	Cl	S
CS 331-1	200-300	< 0.20	< 0.05	< 0.02	< 0.05
CS 331-4	200-300	< 0.20	< 0.05	< 0.02	< 0.05

Zeolite

The term zeolite refers to crystalline aluminosilicate compounds which have well-defined pore structures and geometries. They also contain an exchangeable metal cation and considerable water of hydration as synthesized. By varying the cation and the amount of water present in the structure during manufacturing, the acid/base properties can be somewhat controlled.

Table 2 lists the zeolites received. Their properties are given in Tables 5 and 6. It is possible that the Mobil samples (MCG-7 and 8) are variations of their ZSM-5 zeolite which is used in their second stage MTG reactor. No information was provided by Mobil in this regard, however, so that positive identification is impossible.

Metal oxides

Metal oxides are of particular interest for this application because the acidity and basicity of the catalyst can be easily altered through changes in catalyst formulation. A number of metal oxide catalysts on different supports were received as shown in Table 2. Their properties are shown in Tables 7 and 8.

Ion Exchange Resins

Ion exchange resins have shown low temperature (30° - 150° C) activity for alcohol dehydration [4]. These catalysts are extremely sensitive to both high temperature (> 150° C) and hydration effects, so no testing was undertaken at this time. In addition, the ion exchange resins cannot be formed into monoliths thereby disqualifying them from consideration in this automotive application.

Table 5. Union Carbide Zeolite Catalysts

Catalysts	Composition (wt%) Al_2O_3	SiO_2	Na_2O	NH_3	Remarks
LZ-20	< 40	< 80	< 5		
LZ-M8	-	-	-	< 20	Ammonium Exchanged
LZ-Y-72	< 40	< 80	< 5	-	

Table 6. United Catalyst/Zeochem Zeolite Catalysts

Catalysts	Surface Area (m^2/g)	Al_2O_3	Composition (wt%) $Na_2O \cdot Al_2O_3 \times SiO_2 \times H_2O$	M_gO
United Z6-06-02		25-35	65-75	-
Zeochem Z6-06-02 B6980	375	25-35	65-75	2.4

Table 7. Harshaw/Filtrol Metal Oxide Catalysts

Catalysts	Surface Area m^2/g	Composition (wt%) ZrO_2	TiO_2	Al_2O_3	SiO_2
ZR-0304T	52	980		2.0	0.1
0720	205	-	100		

Table 8. United Catalysts Metal Oxide Catalysts

Catalysts	Surface Area m^2/g	Composition (wt%) Ni	Cu	Cr	Ti	Balance
T-312	183	8-10	10			Al_2O_3
T-314	190	8-10		1.6		Al_2O_3
T-317	187		10-12		0.1-0.2	Al_2O_3
T-1502A	124	15				SiO_2
T-1502B	152	27				SiO_2
		SiO_2	Al_2O_3	Fe_2O_3	CaO	MgO
K-306	250	71.7	12.5	5.2	2.7	3.6

SECTION 3
EXPERIMENTAL

The primary objective of Phase I was to screen and rank a variety of commercially available catalysts with the potential of effecting the dehydration of methanol to dimethyl ether (DME). The minimum requirement of a catalytic dehydration system is to deliver a gas stream of roughly 15 percent DME in methanol to the automobile fuel system under cold start conditions. This corresponds to 30% conversion of methanol by reaction (1). Given that objective and the constraints of available space onboard an automobile, the catalyst must exhibit sufficient activity to produce the required stream in a reactor of feasible size. In addition, to reduce high temperature deactivation, the catalyst must convert approximately 30 percent of the methanol feed at as low a temperature as possible. The rate at which methanol will dehydrate is a function of the reactor temperature and catalyst. Once these are fixed, the extent of conversion of methanol to DME depends on the product of this rate times the time which the methanol spends in contact with the catalyst. This contact time is conveniently given by the liquid hourly space velocity (LHSV). The LHSV is defined as:

$$\text{LHSV} = \frac{\text{the volume of liquid methanol/time}}{\text{the volume of catalyst}} \qquad (3)$$

The overall conversion is then given by :

$$(\text{conversion of methanol in moles}) = \frac{r}{\text{LHSV}} \qquad (4)$$

where:

r = overall reaction rate of methanol dehydration in moles converted per unit time

The reaction rate (r) is normally given in the form of :

$$r = Ae^{-E/RT}\ (C)^n \qquad (5)$$

where:

A = pre-exponential factor which is approximately constant
E = activation energy of the reaction
R = gas constant
T = reaction temperature
C = concentration of the reactants
n = order of reaction

For a given methanol feedstream and catalyst at constant temperature, r can be considered constant. Thus, the conversion of methanol can be increased by decreasing LHSV by Equation (4). Physically, this means that for a given reaction rate, a lower flow rate will permit a higher conversion of methanol. Alternatively, the reaction rate for a given catalyst can be increased dramatically by increasing the reactor temperature, T. The activity of a catalyst is manifested by the activation energy, E. By Equation (5), a lower E has the effect of increasing the reaction rate at a given temperature. Hence, a catalyst that is more "active" exhibits a lower activation and therefore a higher reaction rate for a given temperature, T. Consequently, a more active catalyst will increase conversion of methanol for a given reactor size and capacity (LHSV). Finally, the reaction order (n) can be considered to be equal to one for the heterogeneously catalyzed methanol dehydration reaction as a first approximation.

In the application of onboard methanol dehydration, the total volume of the proposed catalytic reactor must be small. In addition, the reaction is intended to operate under cold start conditions so that a minimum reaction temperature is sought. It should be noted that for a given catalyst this presents a tradeoff in that the lower the reaction temperature, the higher the reactor volume must be to maintain a given level of methanol conversion. The objective of Phase I, then, is simply to identify those catalysts that exhibit the lowest activation energy for the methanol dehydration reaction. These will, in turn, provide the best level of conversion for the minimum reaction temperature and reaction volume.

Experimental Considerations

The rate of a heterogeneously catalyzed reaction of gas phase reactants on the surface of the solid catalyst is determined by the slowest of the following steps:

- ***External mass transfer*** - the rate at which either the gas phase reactants reach or the products leave the surface of the catalyst. This is a function of both the bulk motion of the gas around the catalyst particle as well as the diffusion properties of the reactants and products under the experimental conditions.

- ***Intraparticle mass transfer*** - once the gas phase reactants have reached the catalyst pellet, they must find their way to an active site on the surface. Similarly, after reaction, the products must diffuse away from the active site.

- ***Surface reaction rate*** - Once the gas phase reactant has reached an active site on the catalyst, it must react to form the reaction products. The inherent activation energy describes the rate of this reaction and varies from catalyst to catalyst.

The relative contribution of each of these steps is most easily visualized by considering a varying reactor temperature. Obviously, at very low temperatures.

the reaction rate on the surface is extremely slow and therefore rate controlling. The conversion of the gas phase reactants is limited by the reaction rate on the surface of the catalyst. As the temperature is increased, however, this reaction rate increases (Equation [5]) to the point at which it exceeds the rate at which the reactants reach the surface. Mass transfer is said to be limiting the reaction rate. This resistance could be the rate of reactant transfer from the bulk gas stream to the catalyst pellet (external mass transfer). Most catalysts are porous so that the mass transfer into the pellet pores to the actual surface could also be limiting the overall reaction rate (internal mass transfer). Usually, however, the surface area of the catalyst is large and the particles are small, in which case external mass transfer from the bulk gas stream to the catalyst particle is rate limiting.

In any event, practical systems utilize high reactor temperatures to ensure that the surface chemical kinetics do not limit the production rate. The overall mass transfer of the reactants to the catalyst particle is, therefore, oftentimes the rate limiting step in these heterogeneous systems.

For the purposes of the Phase I screening tests, it was determined to fix as many of the experimental factors as possible so that the evaluation of each catalyst would be under uniform conditions. This need for constancy was effected by a number of experimental considerations each of which will be treated separately.

The LHSV as defined by Equation (3) was kept constant for each catalyst tested. This was done by using the same volume of each catalyst for each test while maintaining a constant methanol volumetric flow rate. In particular, a 0.4 cm I.D. glass tube was packed with catalyst to a length of 4 cm. The volumetric flow rate was constant at 200 cm^3/min of 1,000 ppm methanol in nitrogen. By Equation (3), this equals a LHSV of 6.08 x 10^{-2} hr^{-1} (see Section 6).

Within the catalyst bed, the amount of time that the methanol feed spends in contact with the candidate catalyst should be uniform over the cross-section of the packed reactor. In this study, the candidate catalysts were crushed and sieved to produce a 60-80 mesh size sample (0.18 to 0.25 mm). This was done to minimize non-uniformities in the velocity-profile (and, hence, the contact time) of a gas flowing through the packed bed which can arise due to two mechanisms. The first is simply the diffusion of the species in the axial direction of the flow. For most gases, the ratio of diffusional to convective (or bulk flow) transport increases as the Reynolds number of the fluid in the packed bed decreases. For a given gas flowing above a Reynolds number of 1 [6] this ratio is less than 1. The present system, 1,000 ppm methanol in nitrogen flowing at 200 cm^3/min through a packed bed mean particle diameter of 0.21 mm, has a Reynolds number greater than 2 and is, therefore, in the convective transport

dominated regime, thereby limiting non-uniformity in contact time due to diffusion.

The second mechanism of dispersion in a packed bed reactor is due to a non-uniform bulk velocity profile. In particular, it has been shown that in tubular reactors of small diameter, D_t, with respect to the particle size diameter, D_p, the voidage, or fraction of cross sectional area which is devoid of solid particles, increases dramatically near the wall of the reactor. This effect is due to the interference of the wall with the packing of the solid material. A general criterion states that the ratio of tube diameter to particle diameter should be above 20. In the present case, we have a tube diameter of 4 mm with an average particle size of roughly 0.2 mm resulting a $D_t/D_p = 20$.

Hence, the physical conditions of the experimental microreactor were chosen to minimize the dispersion effects of both axial diffusion and non-uniformities in the bulk velocity profile.

An additional concern of exothermic reactions studies is whether the heat produced by the reaction is sufficient to raise the reactor temperature significantly. In such cases the furnace temperature can read one value while the local catalyst temperature (which is the temperature of the gas at the reaction site) can be somewhat higher. This would lead to inaccurate conclusions concerning the required temperature for a given extent of conversion of the methanol. Since the microreactor was operated in an electrical furnace, it could be assumed that the reactor operated under nearly adiabatic conditions. An estimate of the adiabatic temperature rise across a packed bed reactor is given in Appendix B. Using the values for our system, the temperature rise across the reactor can be calculated to be roughly 53° C for 30 percent methanol conversion when a pure methanol feedstock is used. This would be unacceptably high since that temperature rise could induce further reactions of the DME to subsequent hydrocarbons as described in reaction (2). The same calculation with even complete conversion of a 1,000 ppm methanol feedstream in nitrogen shows an adiabatic temperature rise of only 0.18° C. Hence, it was determined to use a dilute (1,000 ppm) mixture of methanol and nitrogen for the screening test.

Experimental Procedure

Each catalyst was crushed and sieved. The 60-80 mesh cut was calcined in a muffle furnace at 300° C for 1-1/2 hr. A 0.40 cm I.D. pyrex glass tube approximately 62 cm long was used for the reactor vessel. A small amount of glass wool was compressed and forced into the reactor to form the support for the catalyst bed. Sufficient catalyst was then added to form a 4 cm long catalyst bed after gently tapping the sides to induce particle settling. The final mass varied from catalyst to catalyst due to differences in particle densities. Another

compressed plug of glass wool was added to contain the catalyst particles. The glass tube containing the 4 cm catalytic bed was then placed in the reactor furnace and connected to the incoming and outgoing lines. A complete schematic of the experimental apparatus is given in Figure 2.

For the reasons described above, a 1,000 ppm methanol in nitrogen stream was used as the feedstream for this phase of the work. Sufficient back pressure was made available for the system by setting the bottle regulator at 80 psi during each run. The methanol was metered from the bottle through a Tylan FC-260 mass flow valve. The valve was controlled by a Sierra "Flow Box" mass flow controller. The methanol then passed directly to a 10 port gas chromatographic sampling valve (see Figure 3). The sampling valve provided an *in situ* calibrating procedure for the methanol feed stream as follows, (with reference to Figure 3):

First, the methanol coming from the vaporizer (which was not needed in Phase 1 since a gaseous feed stream was used) entered the 10-port-sampling valve. There it was routed through a bypass loop, leaving the valve to be fed to the reactor inlet (see Figure 2). After passing through the catalyst bed, the stream reentered the 10-port-sampling valve as labeled in Figure 3 from the reactor. When the sampling valve was positioned as in the configuration to the left in Figure 3, the stream passed directly to the vent and was routed to the laboratory flue. The sampling valve then switched to the configuration shown on the right in Figure 3. At this time, the helium carrier gas for the gas chromatograph swept the sample out of the bypass loop to the gas chromatograph for analysis. At the same time, the reacted gas stream from the reactor entered the 10-port-sampling valve to be routed through a reactor loop of the same size as the bypass loop and then to vent. While still in this configuration, the unreacted methanol stream from the vaporizer was routed directly to the reactor inlet without passing through the bypass loop. After the bypass gas sample analysis by the gas chromatograph was completed, the valve was switched back to the configuration on the left in Figure 3. Now the helium carrier gas swept the sample out of the reactor loop passing it on to the gas chromatograph for analysis. In this manner, both inlet and outlet streams could be alternately monitored, thereby correcting for daily fluctuations in GC performance.

A Varian Model 3700 Gas Chromatograph equipped with a flame ionization detector (FID) was used for hydrocarbon analysis. Separation was effected by a 1% SP - 1,000 60/80 carbon packed column. The injector temperature, column temperature and detector temperature were maintained at 80°, 60°, and 200° C, respectively. Peak area integration was calculated by a Hewlett-Packard 3392A Integrator. Since each injection of the gas sample to the gas chromatograph required 5 minutes for the complete elution of all the reaction components, the valve was switched every 5 minutes. This was effected by a Hewlett-Packard 19405A Sampler-Event Control Module. Using a prepro-

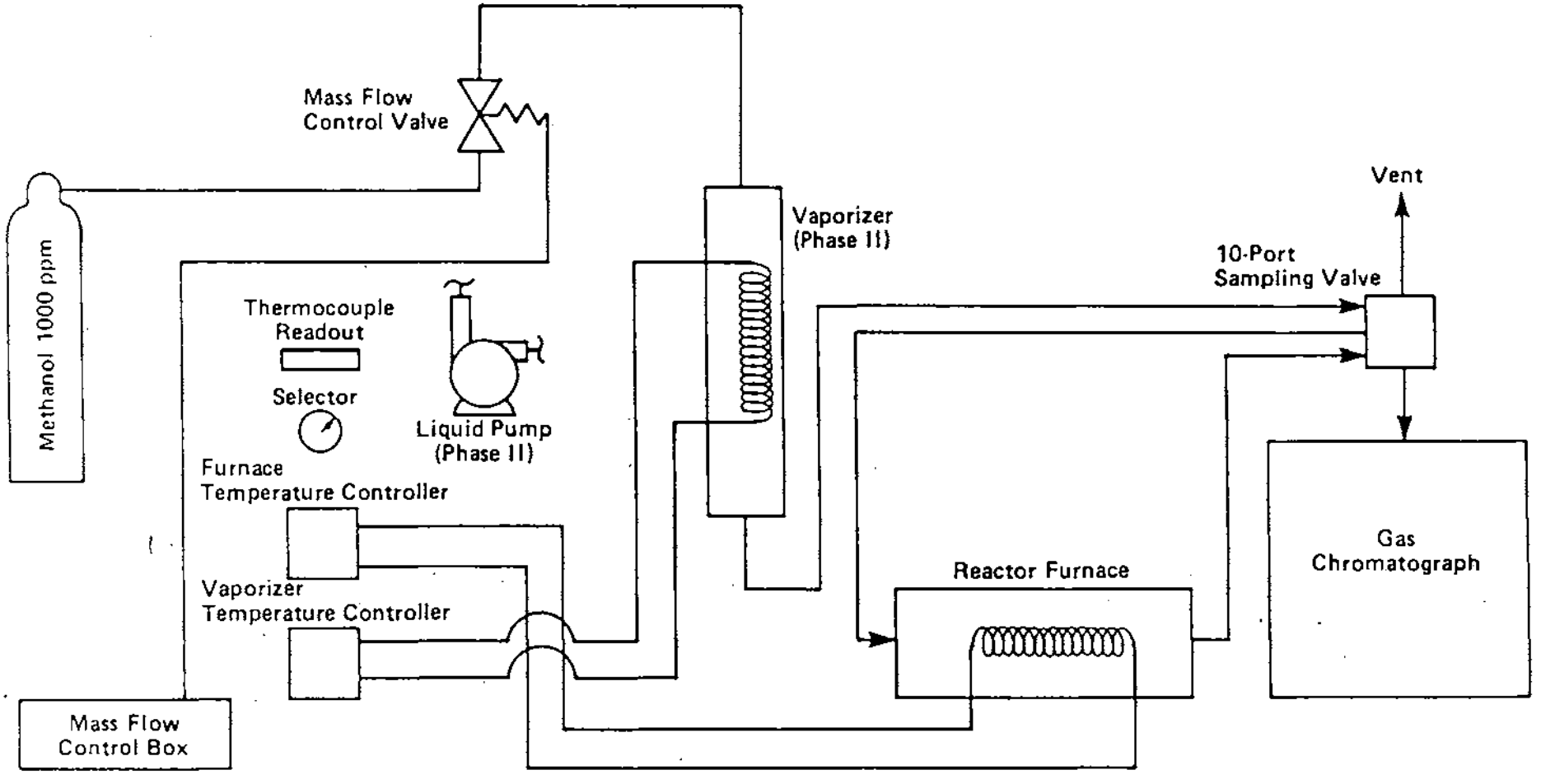

Figure 2. Microreactor catalyst testing facility.

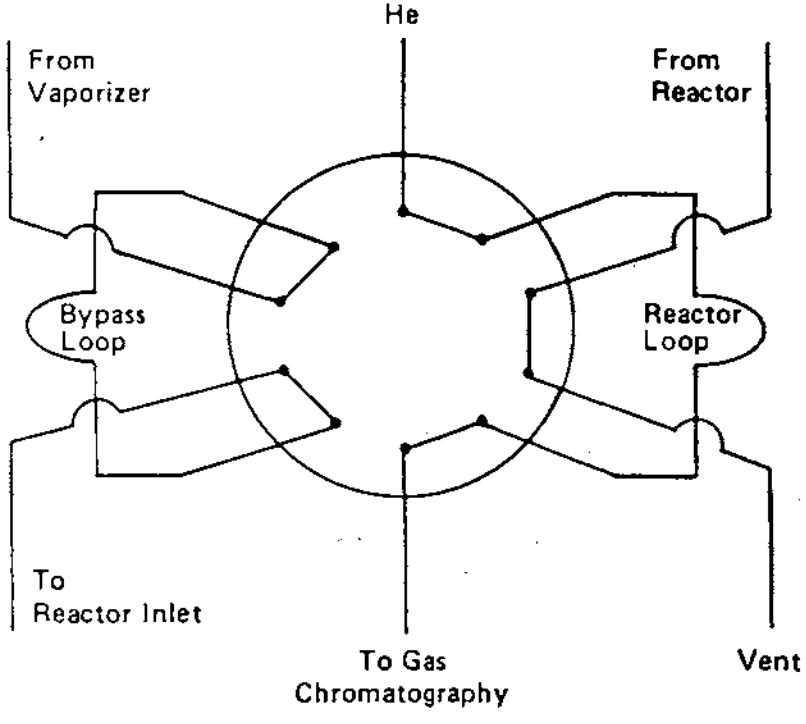

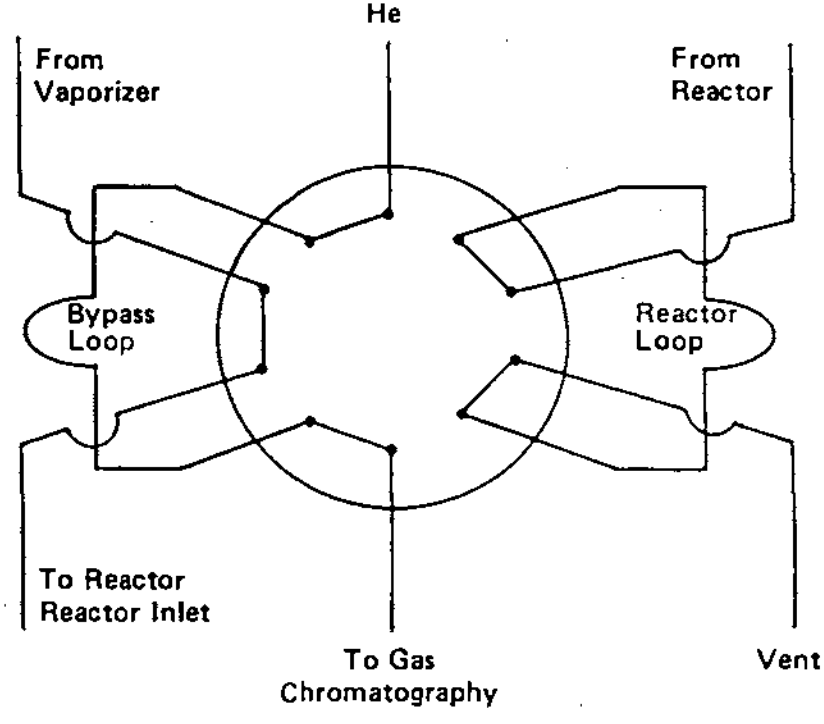

Figure 3. 10-Port sampling valve arrangement.

grammed method, the 3392A integrator controlled the 19405A sampler-event module. The ten-port sampling valve was housed in a Carle Model 4301 Valve Oven configured with a Carle Model 4200 Valve Actuator.

Since the experimental testing required analysis at a variety of reactor temperatures for a given LHSV, a temperature control unit was needed to drive the Thermcraft reactor furnace. To this end, an Omega microprocessor based controller (Model No. CN2011) unit was interfaced with a Tandy 1200 HD personal computer. Software developed by RTI enabled various setpoints to be stored and fed to the Omega temperature controller at timed intervals. For a given set point, the Omega temperature controller brought the reactor furnace to the set point within a ±5° C tolerance. A typical run involved storing a series of nine set points in the computer and beginning the run. Typically the set points were 50°, 85°, 100°,115°, 130°, 150°, 175°, 200° and 225° C. The 50° C run provided a pure methanol output to the gas chromatograph which could be used later for calibration purposes since no reaction occurred at this low temperature. Each set point was maintained for 1 hour during which approximately five samples were taken. Of these, the last three were used for methanol conversion calculations.

After each run, the peak areas calculated by the 3392A integrator were entered in a macro-driven LOTUS spreadsheet with the 50° C input and output methanol peak areas being entered as calibration peaks. The ratio of outlet to inlet areas (in this case, the 0% conversion case) provides a correction factor taking into account the pressure drop across the reactor bed. This is required since the FID is a mass detector rather than a concentration sensitive detector. Hence, the sample stored in the bypass and the reactor loops (see Figure 3) are gases of slightly different densities. Although the reactor and bypass loop volumes are nominally of the same size, different methanol or product masses are injected in each case to the GC. Even when no conversion is occurring across the catalyst bed, the total amount of methanol passing through the flame ionization detector will be less in the case of the reactor loop since the gas there is of lower density due to the pressure drop through the catalyst bed. By entering the input and output peak at 0% conversion (50° C) that ratio can be used to correct the data for the rest of the run since this density difference should remain essentially constant. This was done automatically by the LOTUS spreadsheet.

Once the data were entered, two plots were produced: one showing the methanol conversion as a function of reactor temperature, the other showing approximate concentrations of both methanol and dimethyl ether in the product stream. These plots are discussed in Section 4.

SECTION 4
RESULTS

The results of each catalyst test are presented in a graph depicting the conversion of methanol as a function of reactor temperature. Figures 4 through 10 show these conversion plots for the alumina catalysts tested. Similarly, Figures 11 through 17 present the results for the zeolite catalysts while Figures 18 through 25 present results for the metal oxide catalysts. The equilibrium conversion of methanol to dimethyl ether was shown in the RTI July 1987 proposal to be approximately 90% under these conditions. However, small amounts of DME will react further to higher products, thereby allowing more methanol to be converted.

For selected catalyst tests, a mixture of 290 ppm dimethyl ether in nitrogen was fed to the reactor at room temperature to provide DME calibration areas. Subsequent results could then be represented in terms of actual ppm quantities of methanol and DME in the product stream. These data are shown in Figures 26 through 30 for selected catalysts. An approximate material balance is possible in that,

$$2CH_3OH \rightleftharpoons CH_3OCH_3 + H_2O \qquad (6)$$

produces one part of DME for every two parts of methanol consumed. The data in Figures 26 through 30 are presented in terms of parts per million by volume, so multiplying the DME levels by two and adding them to the methanol level should yield roughly the 1,000 ppm level of methanol feed. At higher levels of conversion, it is likely that some conversion of the DME to higher hydrocarbon occurs which is not detectable at these levels using present equipment. It is significant to note that at a methanol conversion of roughly 30% the material balance is quite accurate, indicating that virtually all the methanol converted at these lower levels forms DME only.

This result can be used to develop a measure to rank the catalysts since a product stream containing 15% by volume of DME in unreacted methanol is required to start an engine under cold start conditions and a 15 volume % DME stream corresponds to 30% conversion of methanol. As the data in Figures 25-30 would indicate, substantially all of the methanol converted at these lower levels of conversion forms DME rather than the higher hydrocarbons with a concomitant formation of coke. Hence, selectivity at these minimum conversion levels is not an important criterion for catalyst selection. The data presented in Figures 4-25 were then used to identify the reactor temperature required to convert 30% of the feed methanol for each catalyst. That temperature, T_{30}, was then used to rank the activity of the candidate catalysts. These results are given in Table 9.

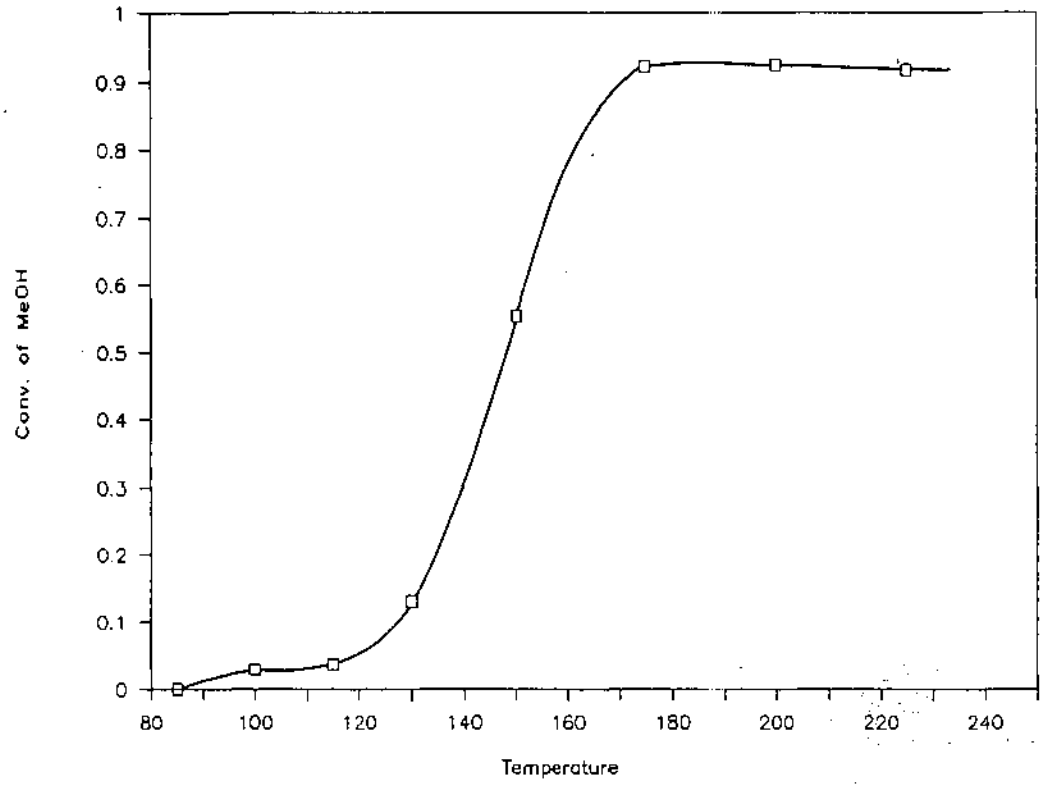

Figure 4. MeOH conversion, AL-5207.

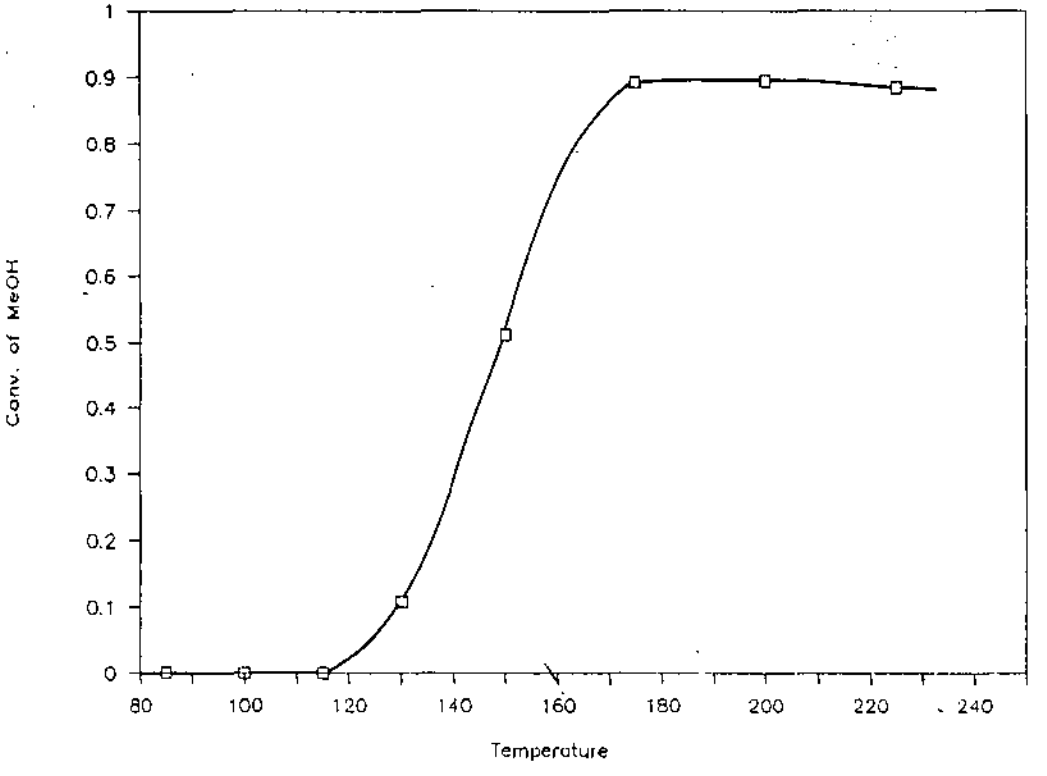

Figure 5. MeOH conversion, AL-5307 E 1/16.

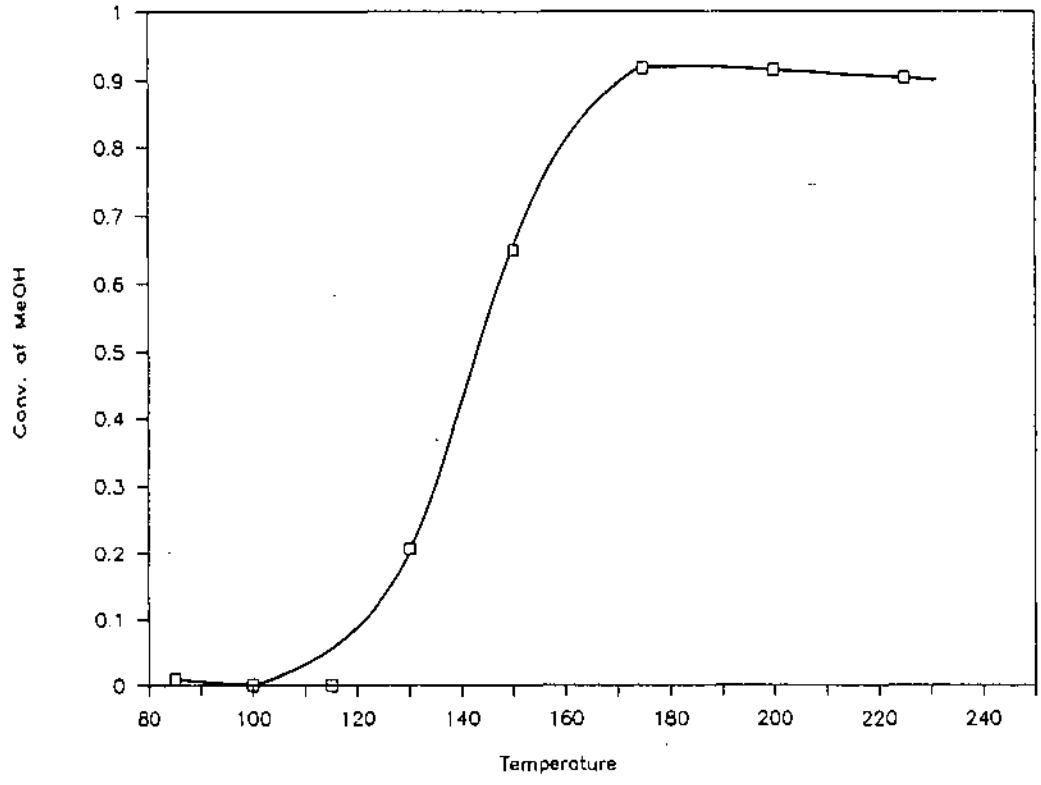

Figure 6. MeOH conversion, AL-5407.

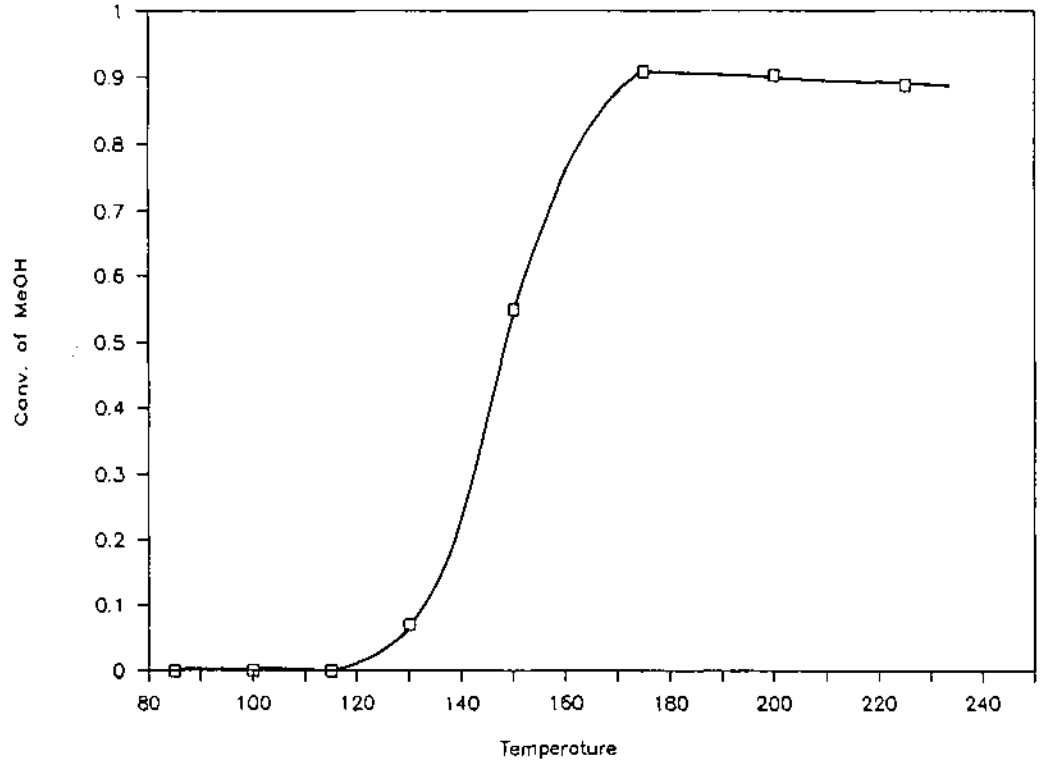

Figure 7. MeOH conversion, AL-3945.

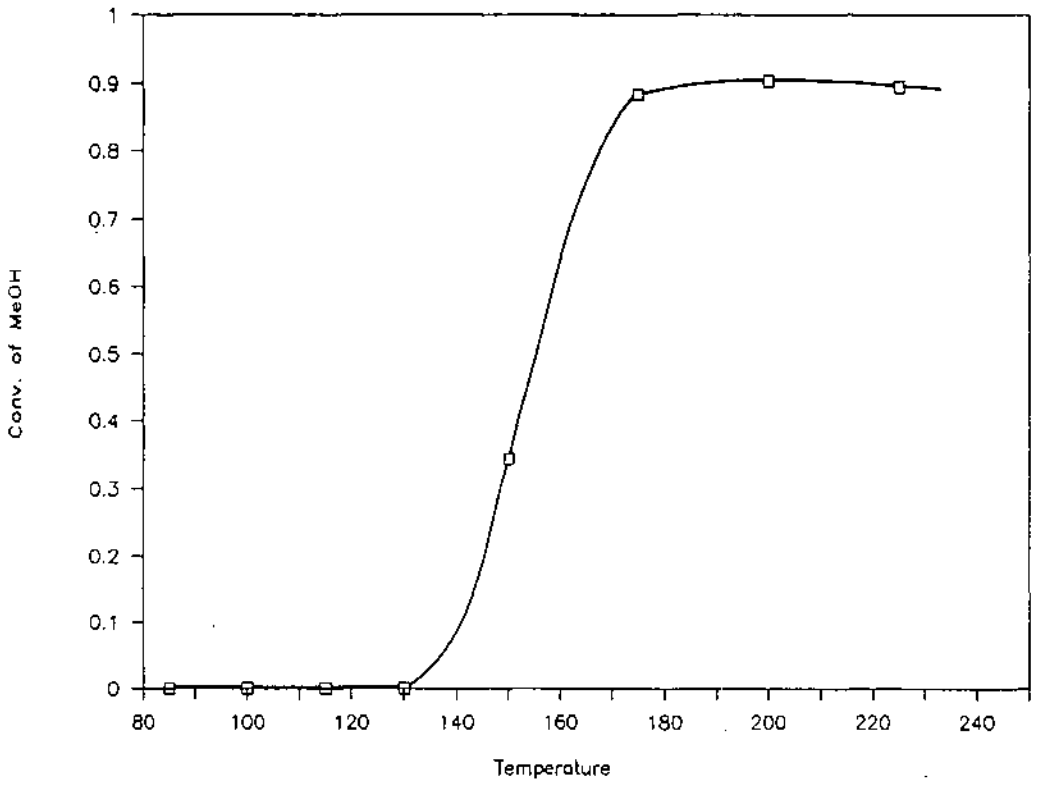

Figure 8. MeOH conversion, AL-3996 R.

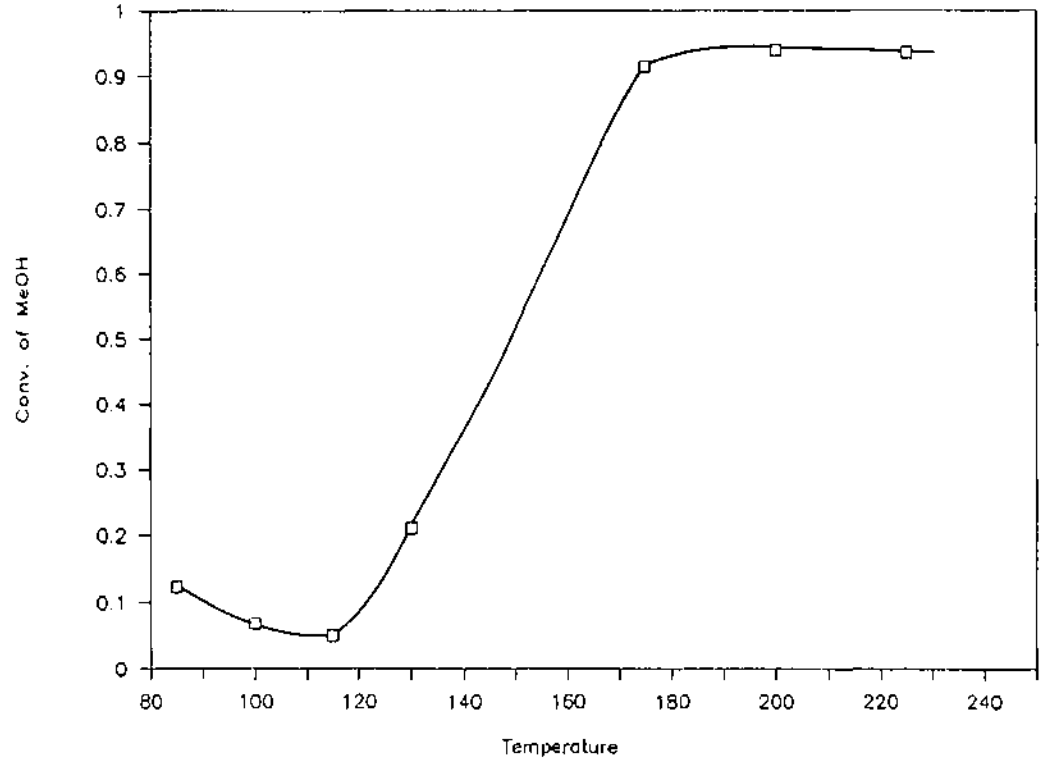

Figure 9. MeOH conversion, CS 331-1.

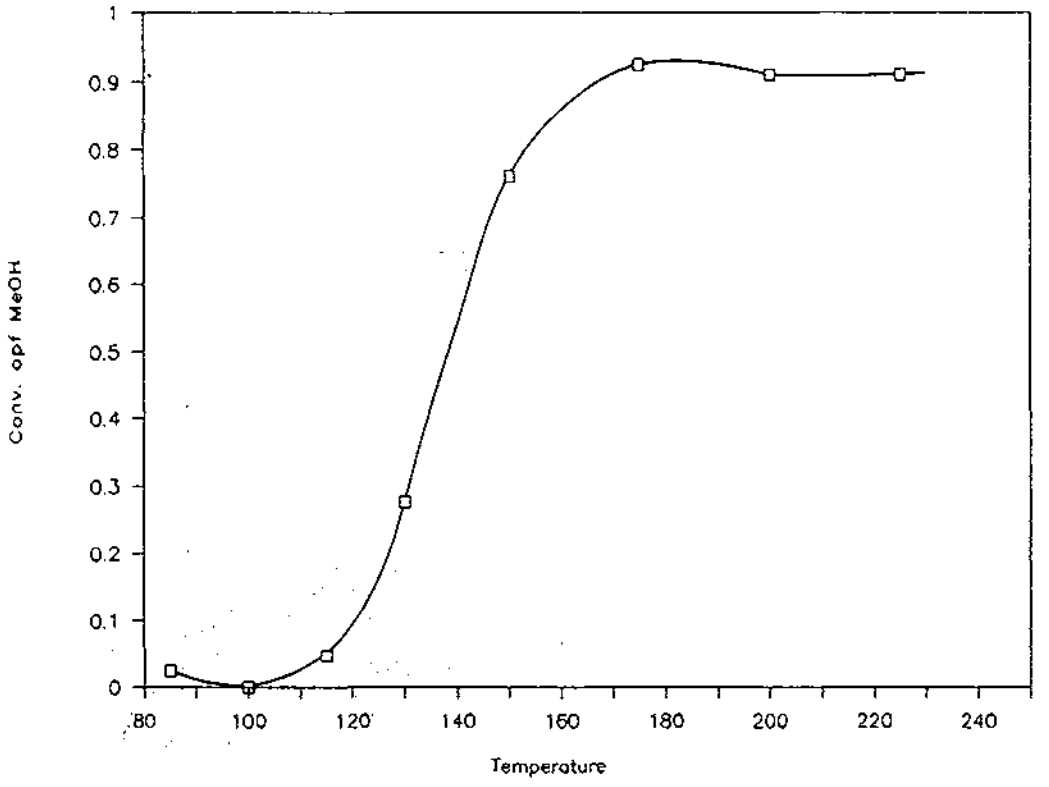

Figure 10. MeOH conversion, CS331-4.

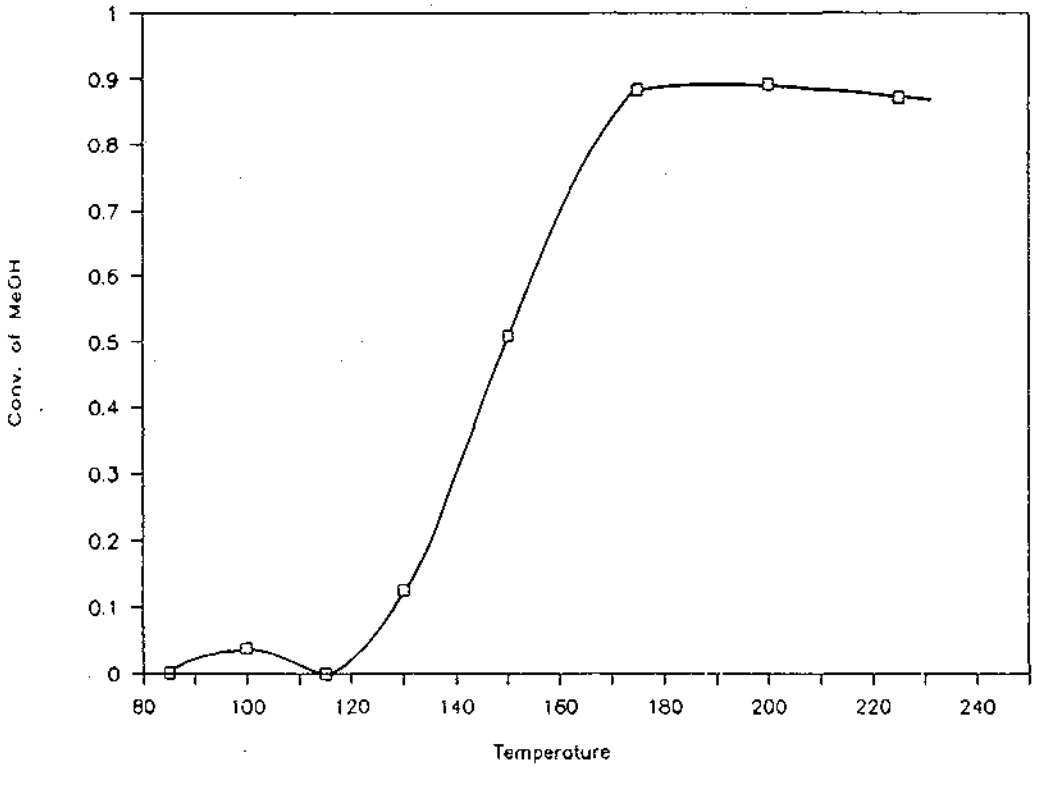

Figure 11. MeOH conversion, LZ-20.

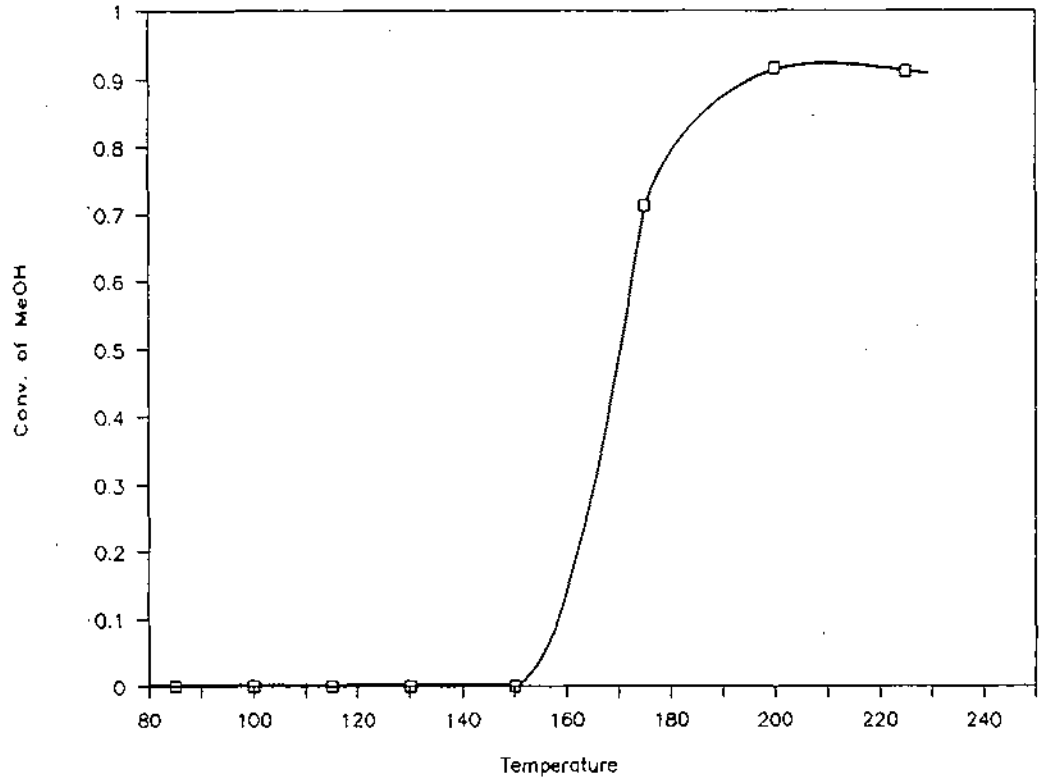

Figure 12. MeOH conversion, LZ-Y-72.

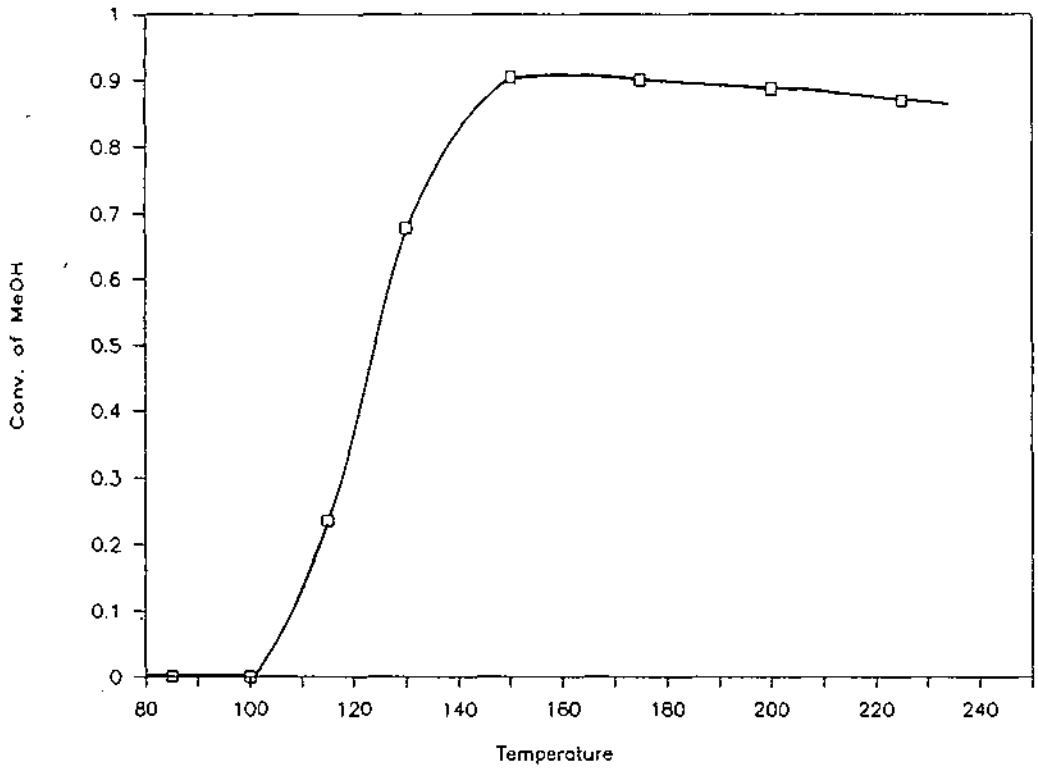

Figure 13. MeOH conversion, LZ-M 8.

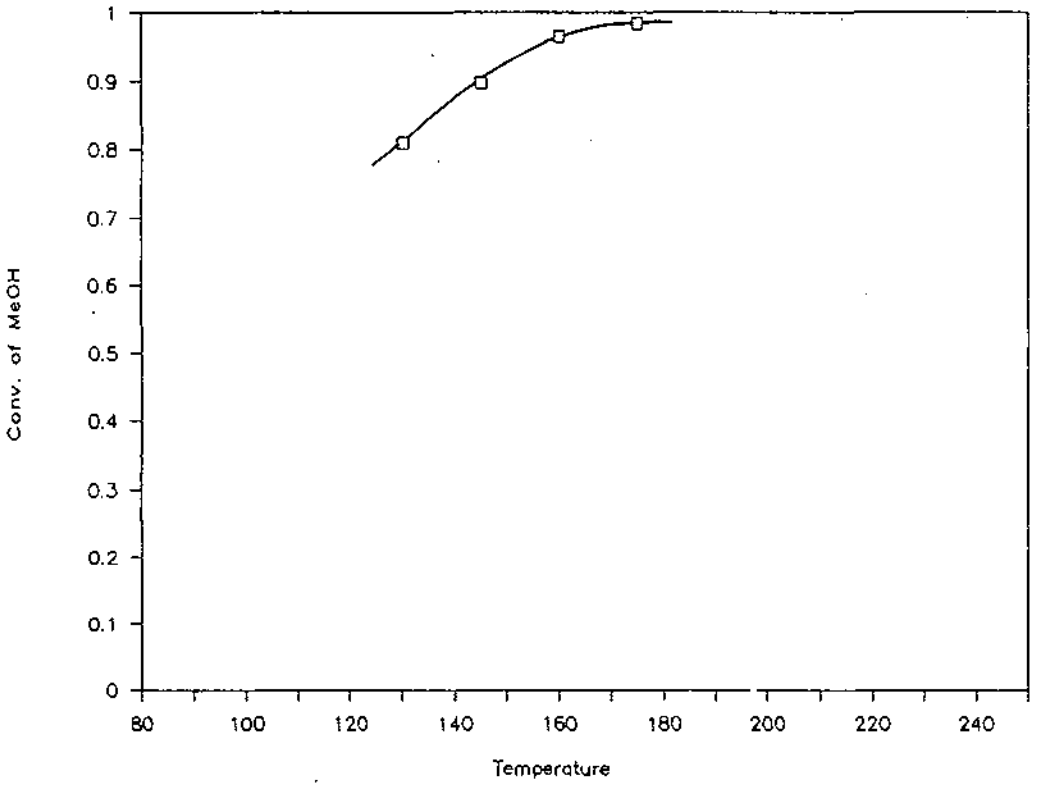

Figure 14. MeOH conversion, Z6-06-02.

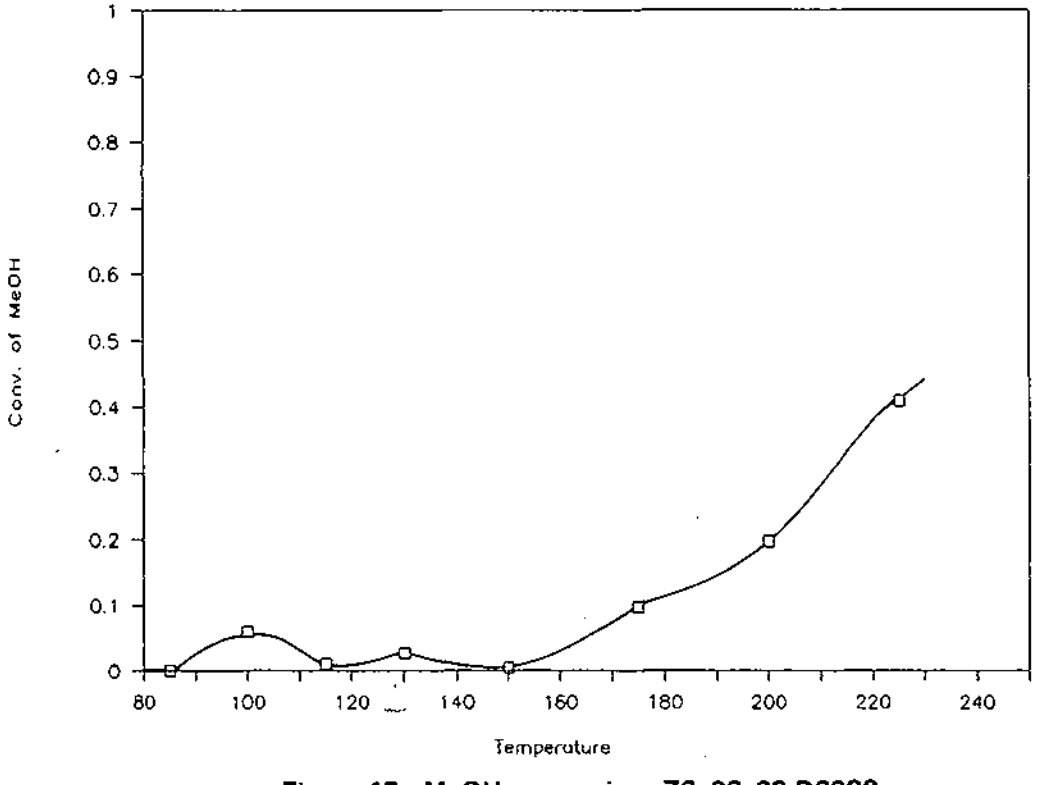

Figure 15. MeOH conversion, Z6-06-02,B6980.

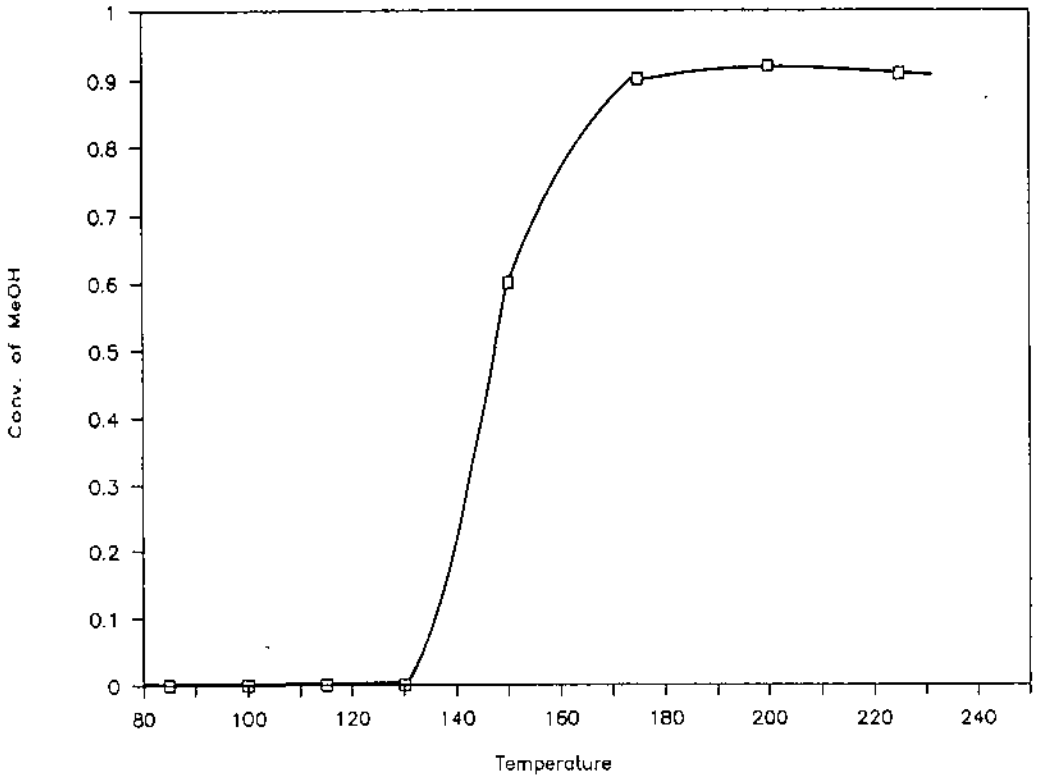

Figure 16. MeOH conversion, MCG-7.

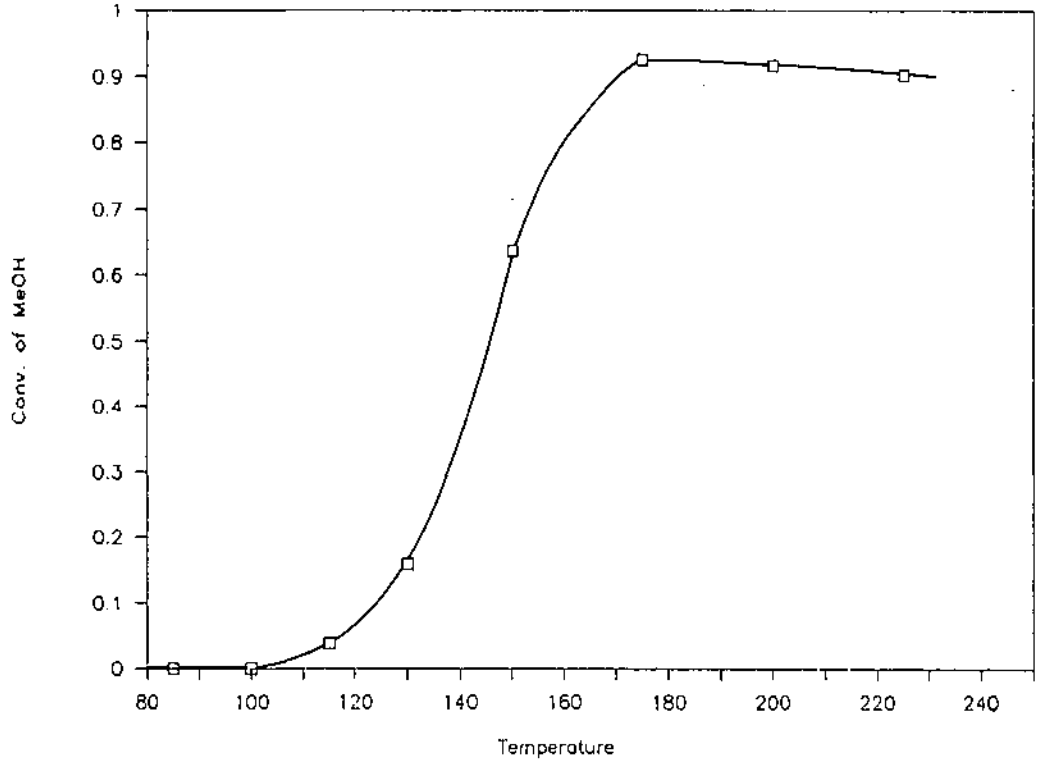

Figure 17. MeOH conversion, MCG-8.

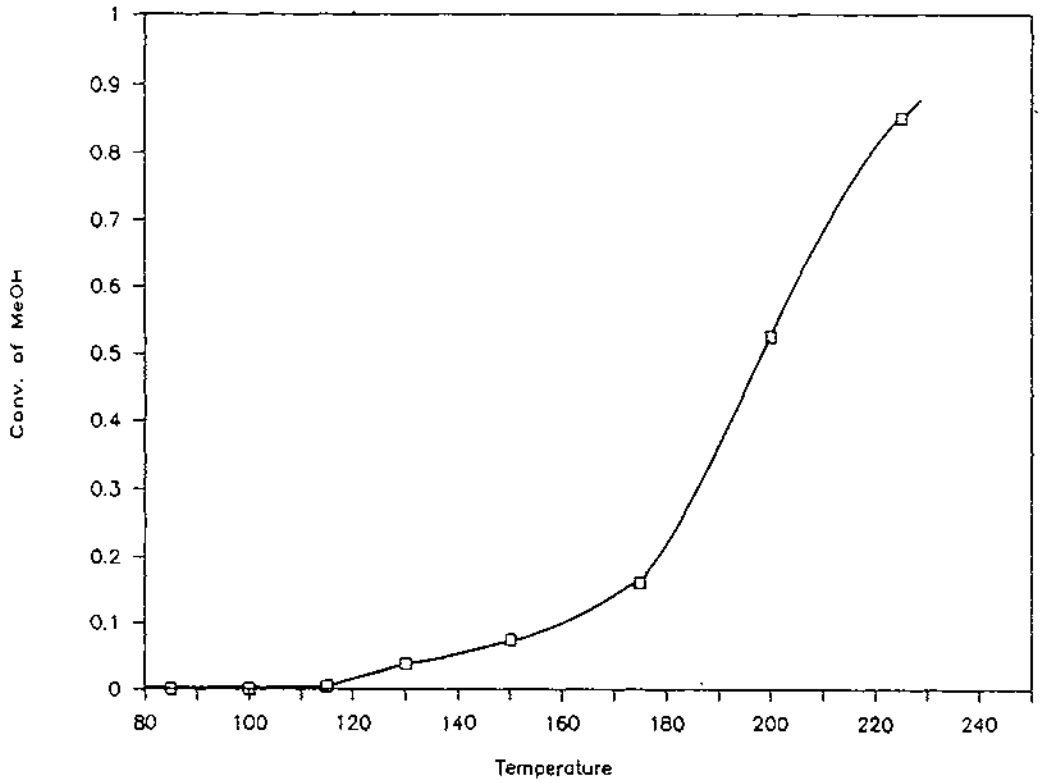

Figure 18. MeOH conversion, ZR-0304T.

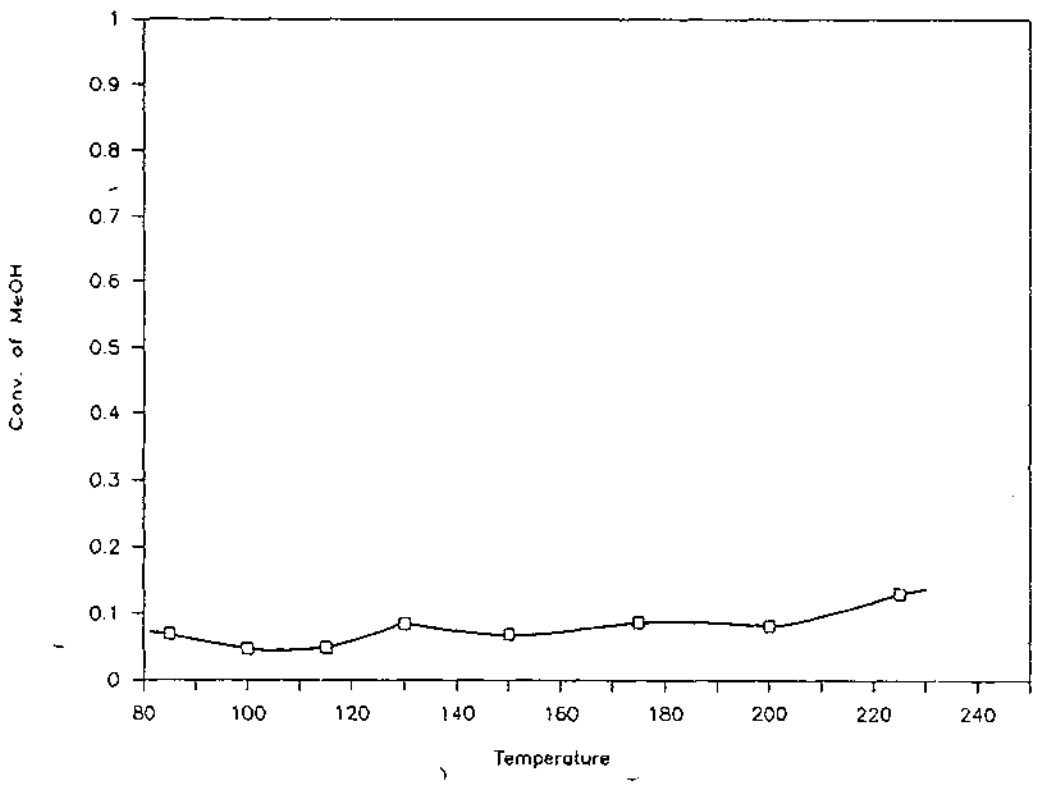

Figure 19. MeOH conversion, TI-0720.

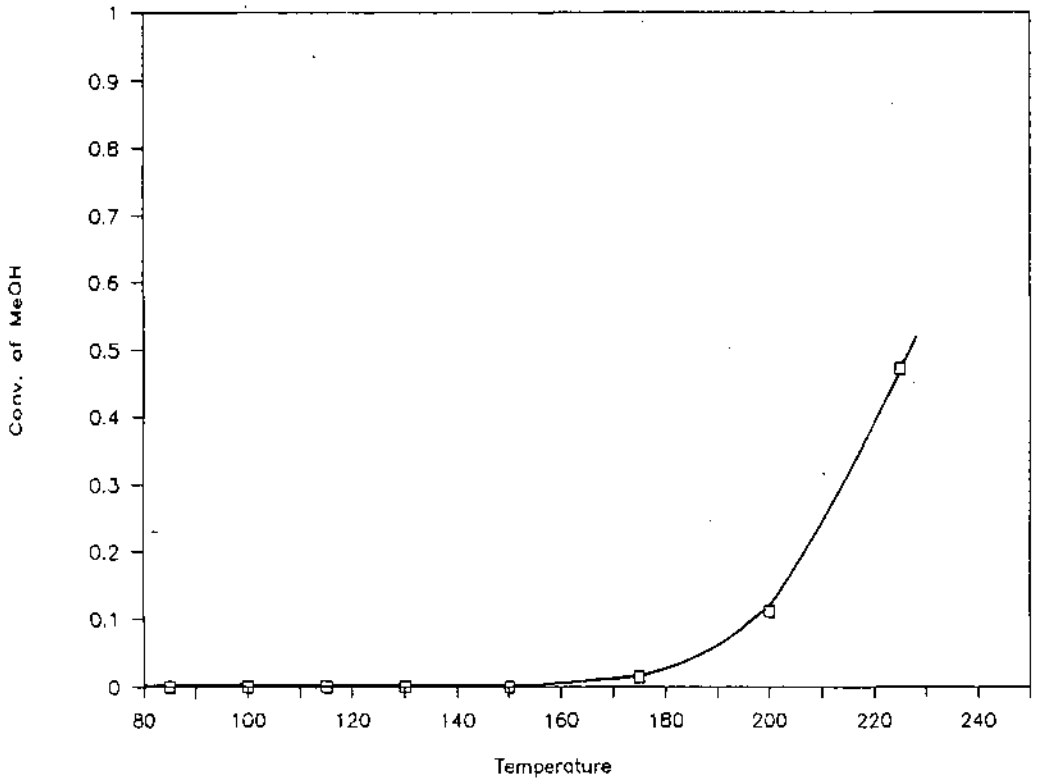

Figure 20. MeOH conversion, T-312.

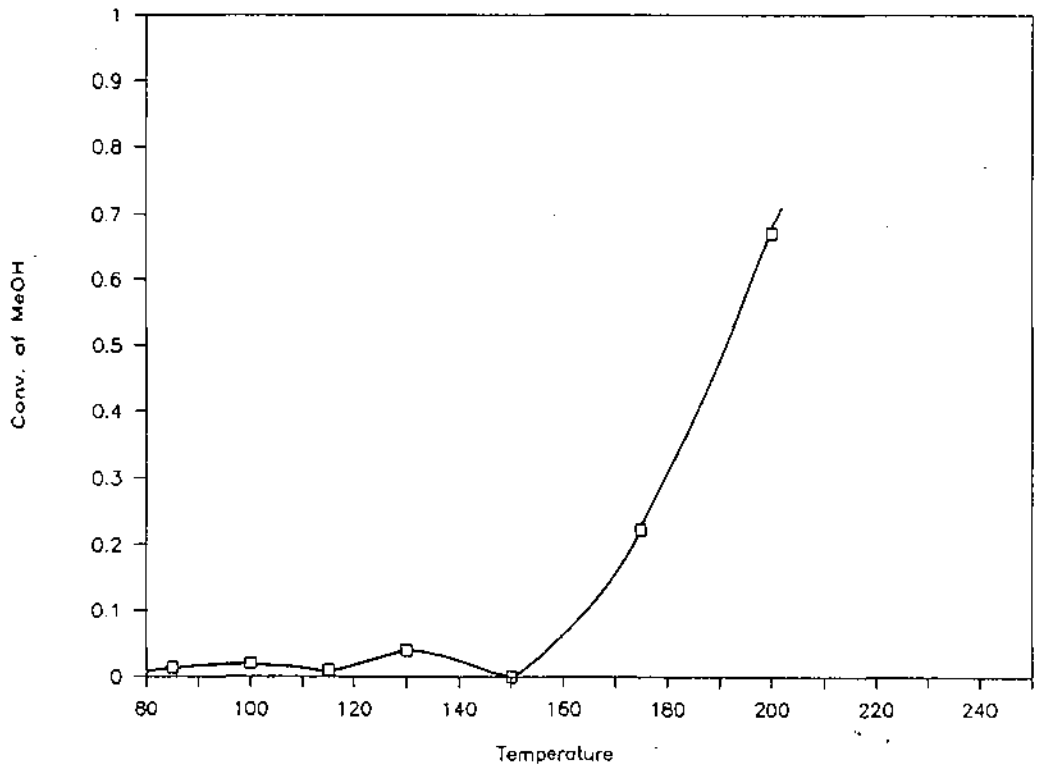

Figure 21. MeOH conversion, T-314.

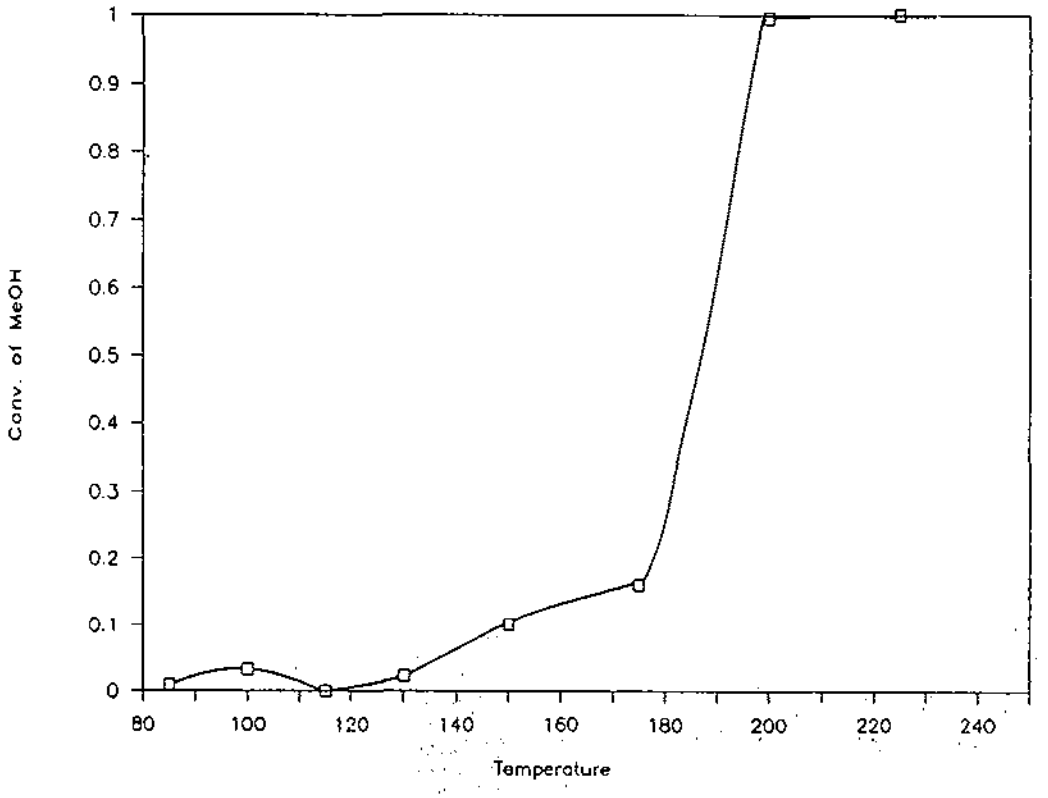

Figure 22. MeOH conversion, T-317.

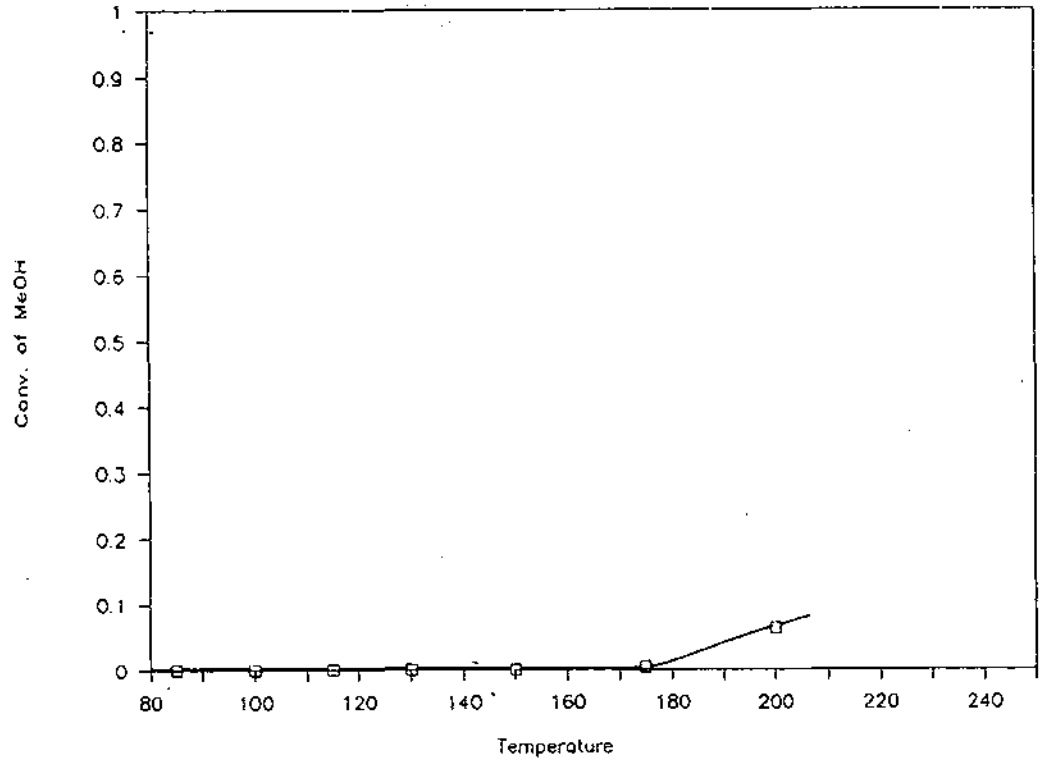

Figure 23. MeOH conversion, T-1502A.

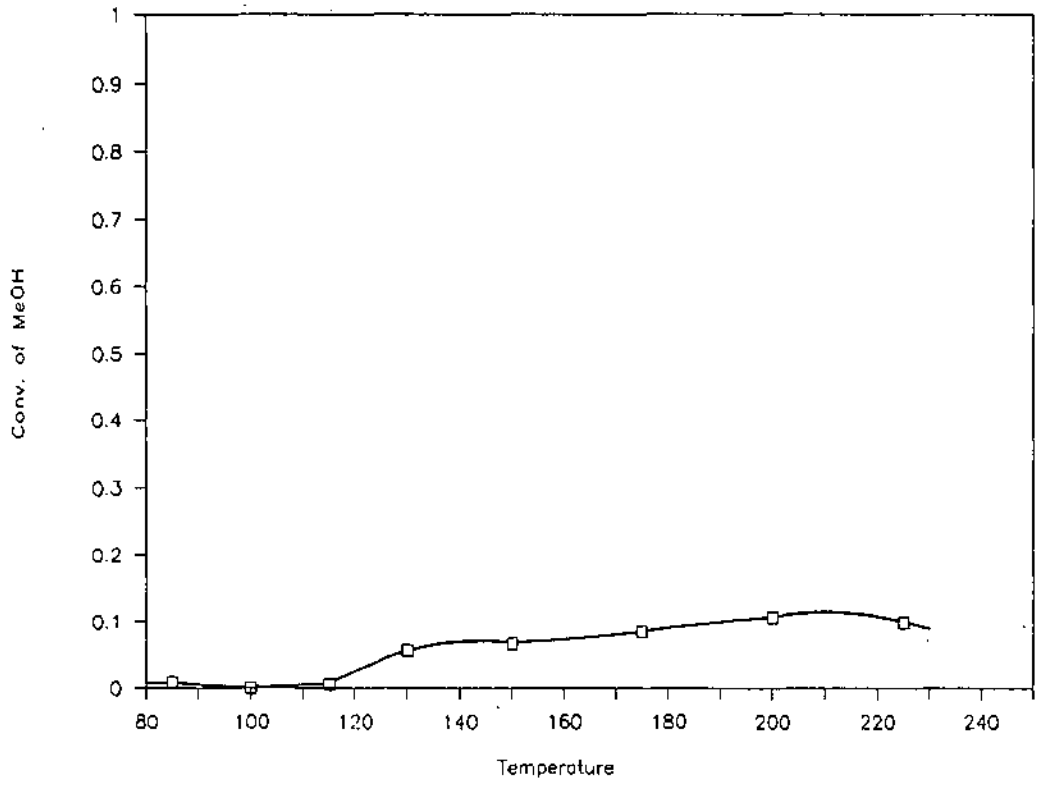

Figure 24. MeOH conversion, T-1502B.

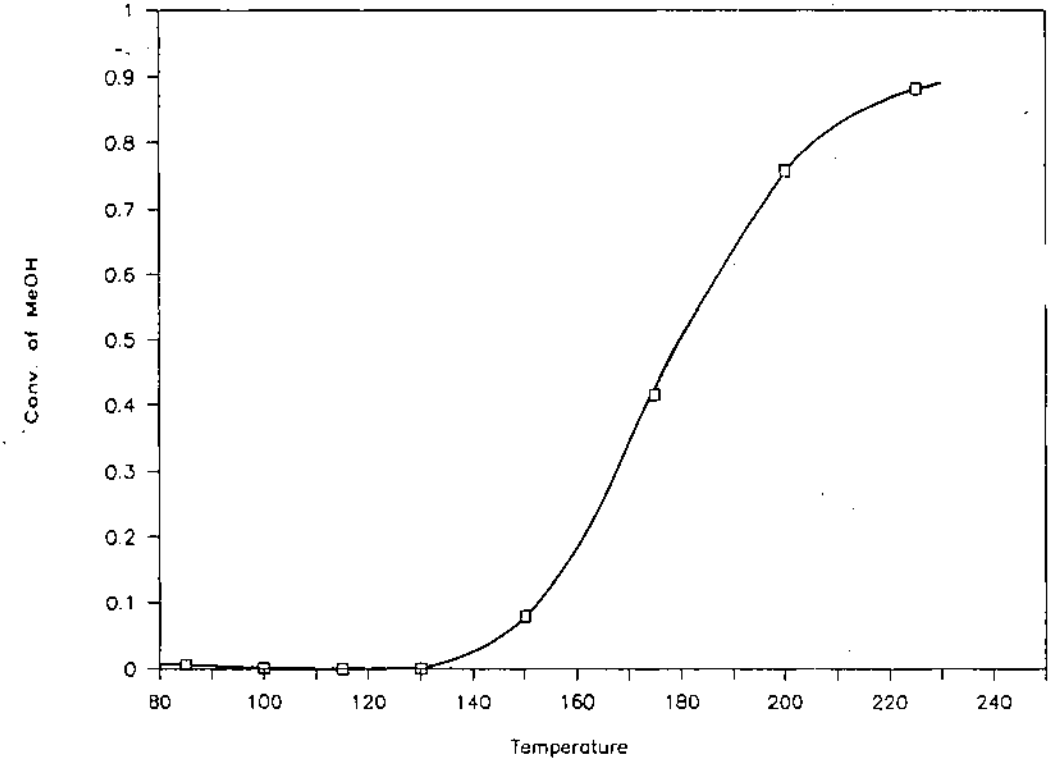

Figure 25. MeOH conversion, 7913-S K-306.

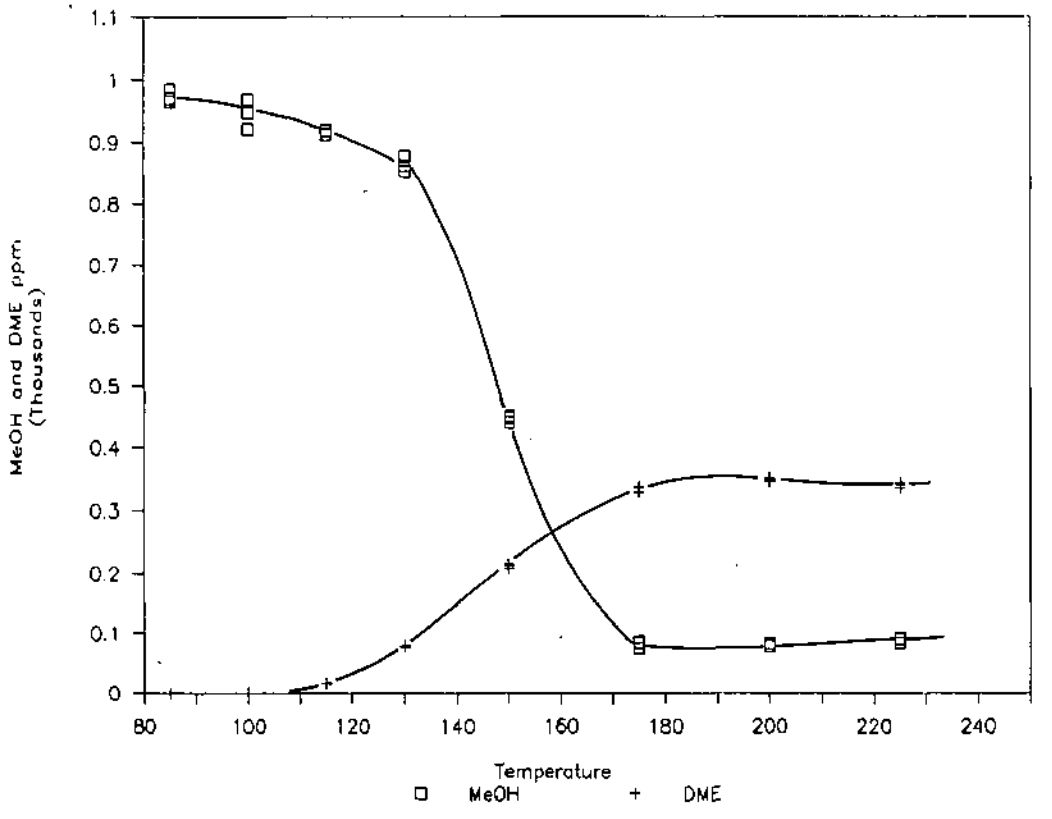

Figure 26. MeOH & DME outputs, AL-5207.

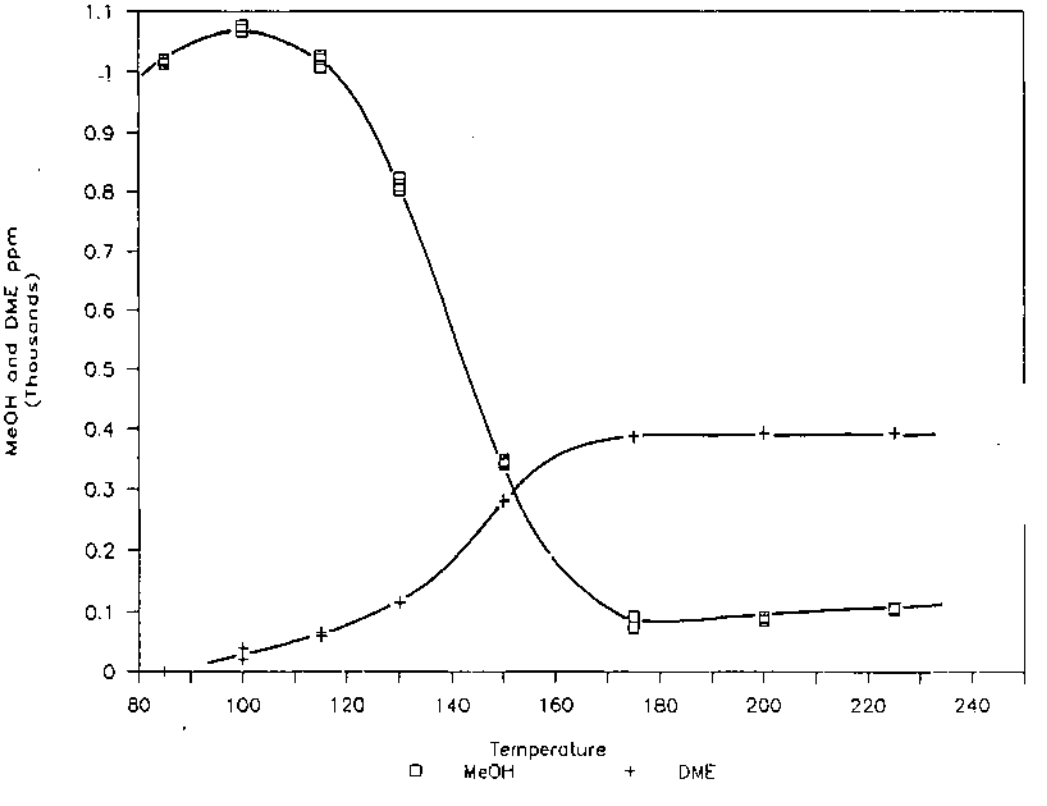

Figure 27. MeOH & DME outputs, AL-5407 E 1/16.

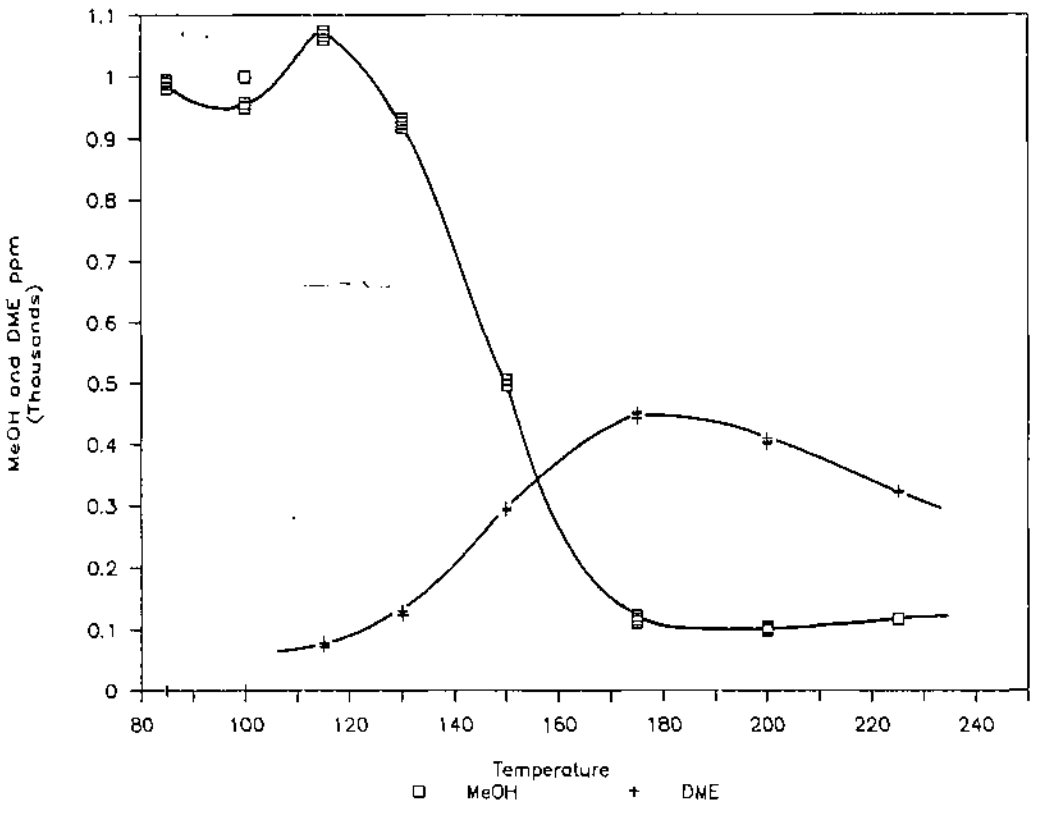

Figure 28. MeOH & DME outputs, LZ-20.

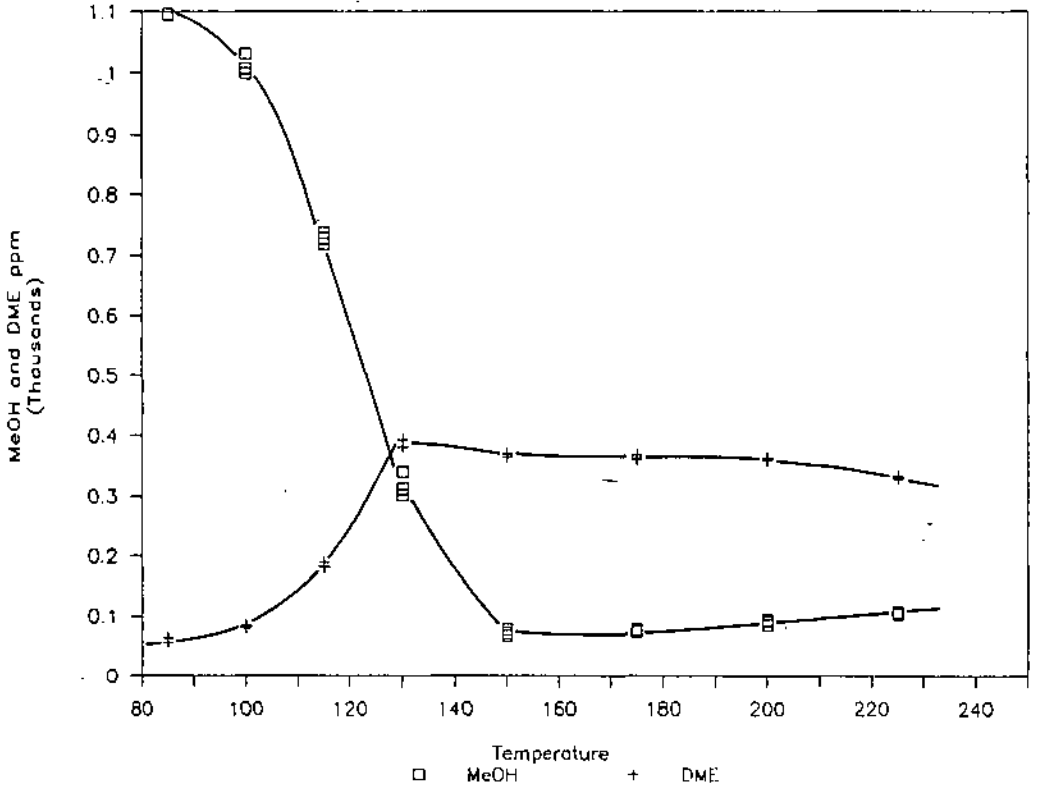

Figure 29. MeOH & DME outputs, M-8.

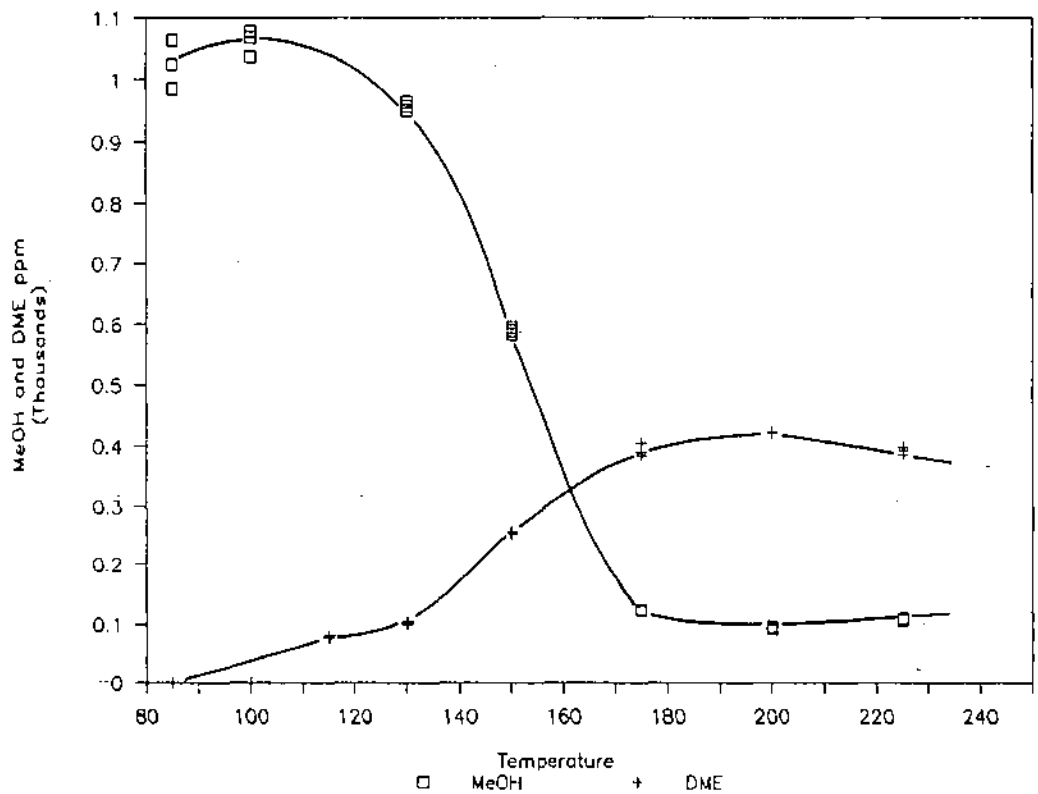

Figure 30. MeOH & DME outputs, Z6-06-02 1/16.

Table 9. Ranking of All Candidate Catalysts Tested According to T_{30}

Catalyst	Catalyst family	T_{30} (°C)
LZ-M8	Zeolite	118
CS-331-4	Alumina	131
AL-5407	Alumina	135.5
MCG-8	Zeolite	136.5
CS 331-1	Alumina	138
AL-5307	Alumina	142
AL-3945	Alumina	142.5
AL-5207	Alumina	142.5
LZ-20	Zeolite	145
MCG-7	Zeolite	145
Z6-06-02	Zeolite	146
AL-3996R	Alumina	148.5
LZ-Y-72	Zeolite	164
7913-S K306	Metal oxide	171.5
T-317	Metal oxide	178
T-314	Metal oxide	186
ZR-0304T	Metal oxide	188
Z6-06-02, B6980	Metal oxide	215
T-312	Metal oxide	216.5
Catalysts Which did not Convert 30% of the Feed Methanol Under the Conditions of the Screening Test		
TI-0720	Metal oxide	
T-1502B	Metal oxide	
T-1502A	Metal oxide	

SECTION 5
DISCUSSION

The results given in Table 9, in which all the catalysts tested are ranked according to their activity for 30% conversion of the feed methanol, are useful in separating some of the candidate catalyst families. In particular, the metal oxide catalysts are less active than either the alumina or zeolite. Even those catalysts in which the metal oxide is supported by an alumina or zeolite (e.g., Z6-O6-O2-B6980) shows significantly higher T_{30} values than their non-metallic counterparts (e.g. Z6-06-02).

It is also interesting to note that the T-317 catalyst showed virtually no methanol (see Figure 20) at higher conversions while all of the other catalysts showed a maximum of roughly 90% methanol conversion. This non-equilibrium value of methanol conversion on the T-317 catalyst indicates that further reaction of DME was occurring. Indeed, upon inspection of the gas chromatographic data some lighter compounds were detected although no identification was made.

Among the aluminas and zeolites no such clear definition exists. The most active catalyst was found to be the ammonia exchanged zeolite M-8 provided by the Union Carbide Corporation. It is known that a mixture of acid and base sites, perhaps provided by the zeolite and ammonia respectively, is necessary for a favorable dehydration catalyst. The alumina catalysts, CS-331-1 and -4 provided by United Catalyst Incorporated are primarily alumina oxide with higher surface area than the Harshaw AL-series (see Tables 3-8). Although the inspection properties of the AL-5207, -5307 and -5407 catalyst are very similar (see Table 3), other literature not reported here shows that the pore volume distribution of the three catalysts are slightly different. In particular, the pore size distribution of the AL-5407 is slightly narrower with the majority of pore volume attributable to pores less than 150 Å. Both AL-5207 and AL-5307 exhibit pores larger than 1,000 Å. Whether this narrow pore size distribution provides a larger number of adjacent sites in the sense of the unimolecular mechanism proposed by Swabb and Gates [5] is unknown. The catalyst literature provided by Harshaw (makers of 5207,5307,5407) does state that this group of alumina catalysts is designed for dehydration reactions. They go on to say that these aluminas have a slightly alkaline nature. Indeed all three of these catalysts provide significant activity.

The catalysts provided by the Mobil Research & Development Corporation (MCG-7 and -8) were sent without literature so that their composition is unknown. It is thought that these are examples of the ZSM-5 catalyst used by Mobil in their MTG second stage reactor wherein the DME is converted to

higher hydrocarbons for gasoline production. No difference between MCG-7 and -8 was indicated by Mobil.

Again, the metal oxide catalysts show a significantly lower activity as evidenced by T_{30} values of more than 20° C above the least active alumina. Of particular note are the T-1502A and B catalysts which are silica supported rather than alumina supported catalysts. Although silica-alumina is highly acidic, silica by itself exhibits no acidity. The titanium oxide catalyst 0720 also has no acidic support and exhibits virtually no activity.

SECTION 6
PHASE II PLAN OF WORK

In light of the data presented as Phase I of this contract it is likely that a suitable commercial candidate exists for the initiation of Phase II. The goal of this phase is the design and construction of a prototype dehydration reactor capable of providing a combustible mixture of methanol and DME (> 15% vol. DME) at a mass flowrate sufficient to start a spark-ignition engine. Calculations (see Appendix C) show that if an energy flow of 6 kcal/sec is needed to start an engine, a volumetric flowrate of liquid methanol of roughly 89.8 cm^3/min must be fed to the dehydration reactor. This value can be used in a simple reactor design. A practical constraint on the design of the prototype is one of size. The need to mount this unit in the engine compartment of most vehicles limits total reactor volume. To illustrate this point a maximum unit size will be assumed as a tube 10 cm I.D. and 35 cm in length. If the catalyst were to occupy 70% of the internal volume of this reactor, its LHSV is

$$\text{LHSV} = \frac{5388 \text{ cm}^3 \text{ (liquid methanol)}}{\text{hr } (0.70)(\pi)(5 \text{ cm})^2 (35)} \tag{7}$$

$$= 2.8 \text{ hr}^{-1}$$

This should be compared with the LHSV of the microreactor system used in Phase I:

$$\text{LHSV} = \frac{\frac{200 \text{ cm}^3}{\text{min}} \; \frac{60 \text{ min}}{\text{hr}} \; \frac{1000 \text{ cm MeOH}^3}{10^6 \text{ cm}^3 \text{ total}} \; \frac{\text{mol}}{22{,}400 \text{ cm}^3} \; \frac{\text{cm}^3 \text{ (liq)}}{0.025 \text{ mol}}}{(0.70)\ (\pi)\ (.2 \text{ cm})^2\ (4 \text{ cm})}$$

$$= 6.08 \times 10^{-2} \text{ hr} \tag{8}$$

It is seen that a LHSV of more than two orders of magnitude greater than that used in Phase I will be needed in the prototype. For 30% conversion, the feed methanol will have to be at a higher reactor temperature. Referring to the data published by Chang et al. [1] shown in Figure 1, the space time (1/LHSV) required for the prototype ($1/2.8 \text{ hr}^{-1} = 0.36$ hr) is greater than the space time needed for 30% conversion (roughly 10^{-3} hr) measured by those investigators. This means that the temperature, T_{30}, for the prototype unit must be higher than the 150° C measured in the Phase I but lower than the 371° C studied by Chang et al.

Some problems exist in simply raising the reactor temperature for 30% conversion at the higher LHSV in the prototype. The methanol dehydration reaction is considerably exothermic. Therefore, the heat that evolves during the conversion of methanol in the reactor must be carried away at a sufficient rate to prevent a significant rise in the reactor temperature. Otherwise, the higher temperature will raise the reaction rate and, consequently, the heat of reaction, which thereby liberated, leads to yet higher temperatures. The maximum temperature, T_{ad}, is that which would result in an adiabatic system and can be calculated using a standard expression as given by Kramers and Westerterp [7]. The calculation (given in Appendix D) shows that T_{ad} would equal 377° C.

Thus, if the prototype reactor is allowed to operate adiabatically, the gas phase temperature will rise approximately 177° C over the length of the unit. Exactly where the rise will occur is not readily calculated although some approximate results will be discussed shortly.

The selectivity of the methanol dehydration will suffer dramatically if such a temperature rise occurs. It was shown in equation (7) that the LHSV required to start a cold engine is 2.8 hr^{-1} or a space time (1/LHSV) of 0.36 hr. This is much longer than the approximately 10^{-3} hr Chang et al. used to achieve a 30% conversion of methanol at 371° C on ZSM-5. Hence, a significantly lower reactor temperature would suffice in the case of the automobile prototype (say, 200° C). If, on the other hand, such a unit experienced a 177° C temperature rise at its midpoint, the remainder of the reactor would operate at 377° C. The space time for this reactor would be $0.36 \div 2 = 0.18$ hr. From Figure 1, a reactor operated at 371° C and space time of 0.18 hr will produce primarily higher hydrocarbons. This, in turn, will lead to significant coking with subsequent catalyst deactivation.

Of course, the prototype will not be operated adiabatically. The temperature rise of the gas phase reactants will then depend on a balance between the rate of heat production (via reaction) and the rate of heat transferred away from the reactor. Probably the simplest configuration of such a non-adiabatic methanol dehydration reactor is shown below:

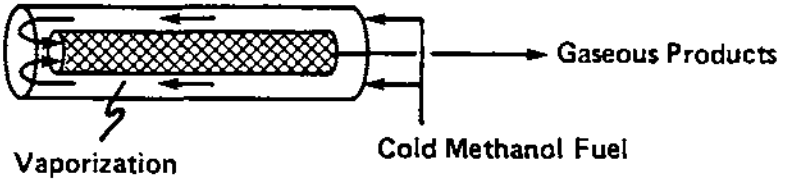

This reactor utilizes the methanol fuel as a coolant while vaporizing and preheating it as reactant to the dehydrator. The heat requirements for this process will be described below. For now, however, it is important to focus on the reactor itself. Gaseous methanol will enter at a temperature of roughly

200° C. The dehydration reaction will be initiated thereby generating heat. It was shown above that a temperature rise of 177° C is possible with no heat exchange resulting in the rapid deactivation of the catalyst. As the rate of heat exchange is increased (from zero), however, the maximum temperature, T_{max}, reached in the reactor will drop. At sufficiently high values of heat transfer, the reaction will proceed in a controlled fashion resulting in prolonged catalyst life and proper product selectivity. It has been shown [8] that the transition from controlled operation (with small T_{max}) to a rapid and severe temperature rise (with large T_{max}) is a critical phenomenon. Bilous and Amundson [9] demonstrated the profound effect small changes in the coolant stream temperature had on the gas phase temperature in an exothermic reaction system (see Figure 31). The region of parameter sensitivity can be estimated without resort to an exact solution of the relevant heat and mass balances by a method due to Barkelew [10]. This analysis showed that a relationship between two dimensionless parameters exists which defines the region of reactor sensitivity. The first of these parameters is defined as,

$$N_{ad} = \left[\frac{E}{RT_c^2} \right] \left[\frac{\Delta H_r}{C_p} \right] \tag{9}$$

which is related to the adiabatic temperature rise (see Appendix B). Here T_c is the coolant temperature. The second parameter describes the cooling (heat transfer) capacity of the system.

$$N_c = \frac{2U}{k_v \rho C_p R_t} \tag{10}$$

where k_v is the rate constant as defined in Appendix D, ρ is the gas density, C_p is the specific heat capacity, U is the overall heat transfer coefficient and R_t is the radius of the tubular reactor. The relationship between these two dimensionless parameters is shown in Figure 32.

Using the kinetic data calculated in Appendix D, the values of these parameters may be computed for the prototype system. The following values will be used:

$E = 2.7 \times 10^4$ cal/mol
$\Delta H_v = -2.2 \times 10^3$ cal/mol
$C_p = 12.4$ cal/mol K
$R = 1.987$ cal/mol K
$T_c = 375$ K
$U = 5.4$ cal/cm^2 hr.K
$k_v = 1.2 \times 10^4$ cm^3/cm^3 hr (at 140° C)
$\rho = 9.92 \times 10^{-4}$ g/cm^3
$R_t = 5$ cm

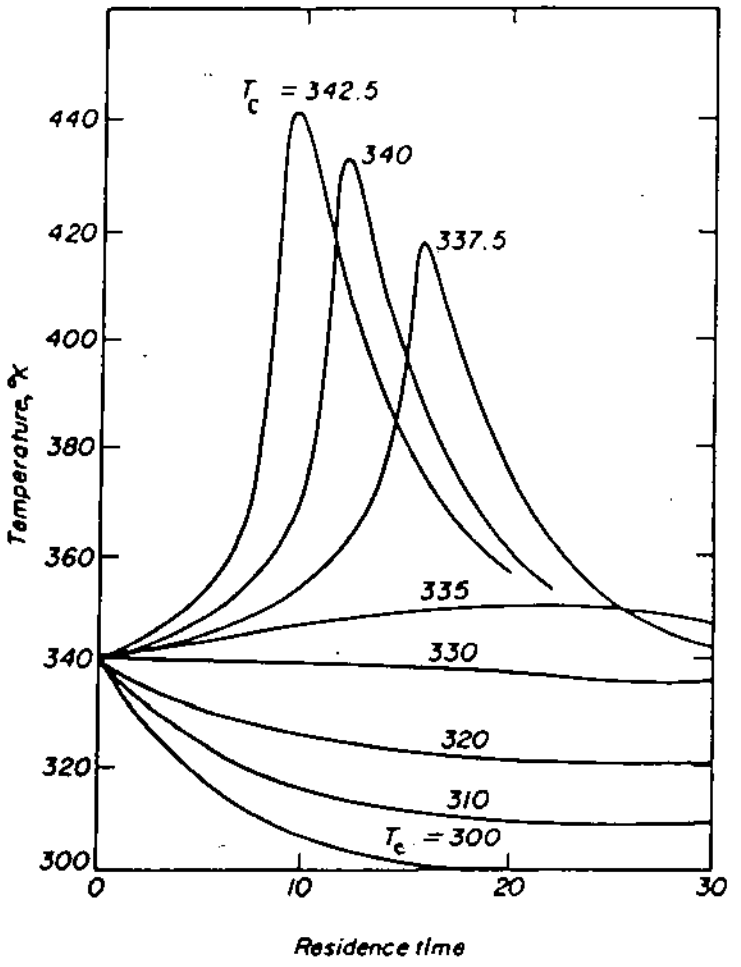

Figure 31. Effect of T_c on the temperature profile of a PFTR [9].

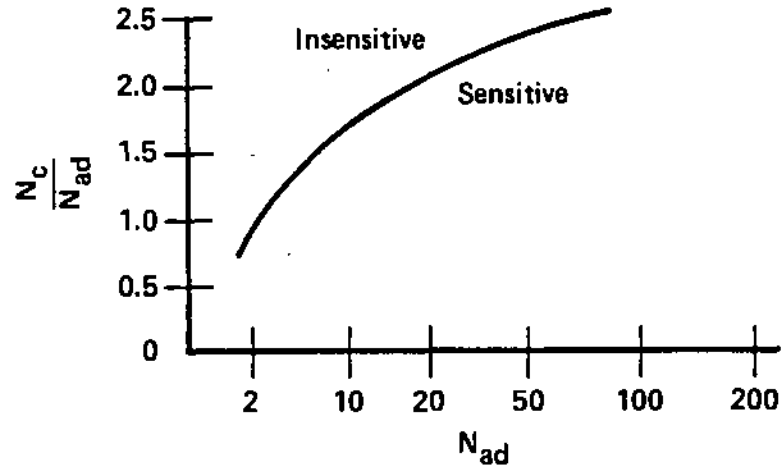

Figure 32. Relationship between two dimensionless parameters.

Note the assumed coolant temperature, T_c, of 102° C. This temperature will vary in the reactor configuration shown in Figure 5, from the boiling point of methanol, 65° C, to the reactor inlet temperature. This latter value was assumed to be 140° C. T_c was assumed to be the average of these two or 102° C. Using these values,

$$N_{ad} = 17$$
$$N_c = 0.47$$
$$N_c/N_{ad} = 2.8 \times 10^{-2}.$$

This value is clearly in the sensitive region in Figure 32 indicating that a runaway temperature excursion is possible.

The reactor system described by the above values must be changed. Unfortunately, not all of the parameters that make up N_{ad} and N_c are controllable. In particular, U/R_i and k_v could be effectively varied.

The overall heat transfer coefficient, U, describes the heat transfer from the reacting gas through the reactor vessel to the coolant medium (in this case, liquid methanol). The rate limiting step in this exchange is that of the gas to reactor vessel. While little can be done to improve this rate, using the reactor configuration shown in Figure 31, the surface area over which the heat is transferred can be increased. That is, R_i can be decreased. In fact, even if ten 3.2 cm I.D. reactors were used in a shell and tube arrangement (i.e. ten tubes surrounded by the liquid (boiling) methanol all housed in a larger diameter vessel), N_c would only be increased to 1.5. The ratio of N_c/N_{ad} would only be 9×10^{-2} which is still clearly in the sensitive region.

Alternatively, a less active catalyst could be used thereby reducing k_v and decreasing N_{ad}. Equation (D.7) shows, however, that a decrease in k_v would require an increase in V_{cat} for a constant level of conversion and feedrate thereby requiring a larger reactor vessel. This would be unacceptable from a volume standpoint.

Apparently a more sophisticated reactor design would be required to improve U in N_c in an effort to de-sensitize the dehydration reactor. A number of options exist, one of which would be a series of tubular reactors with interstage cooling.

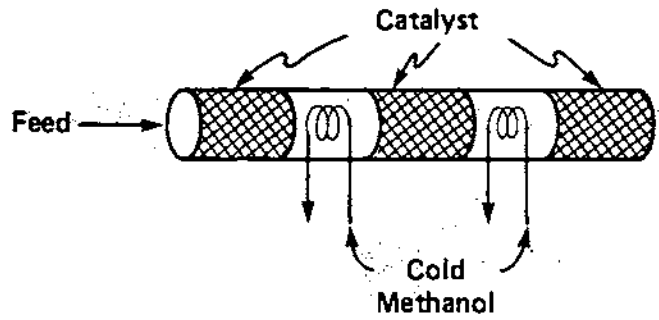

Here, each reactor stage allows the gas phase temperature to rise due to the heat of reaction. Before the temperature reaches a point which would degrade product selectivity and catalyst life, however, the reactants pass through a non-catalyst cooling section before entering a second reactor stage. The temperature history of the gas-phase reactants would be

As the concentration of methanol decreases along space (or time), the space (or time) needed to reach the maximum allowable temperature will increase. Thus, proper design would provide increasingly longer reactors.

It should be noted that the optimization of any reactor design will require some mathematical modeling of the reaction network and reactor system. This will require some limited kinetic data which can be obtained using the present microreactor apparatus already operational. By operating in a low conversion ("differential mode"), initial rate data can be measured relatively easily. This data can then be used in conjunction with the appropriate reactor model to evaluate its optimal design.

Dissociation Reaction

In the case of the exothermic dehydration reaction, it was shown that the system could develop a runaway temperature excursion detrimental to both product selectivity and catalyst life. To maintain a (parameter insensitive) system, however, a completely novel reactor concept may be sought. One such concept, originally brought forth by the U.S. Environmental Protection Agency (EPA), uses an endothermic catalytic reaction which could provide an *in situ* heat sink to limit a temperature excursion. The methanol dissociation reaction,

$$CH_3OH \rightleftharpoons CO + 2H_2 \qquad (11)$$

is a highly endothermic reaction yielding CO and H_2. These products are suitable for cold starting combustion requirements in that they are volatile and have high octane values. Work previously by EPA dealing with this reaction for a different application has identified a dissociation catalyst with favorable properties. Preliminary work with this catalyst was performed using the same equipment and procedure discussed in Section 3. A 4 cm bed of this dissociation catalyst was found to have a T_{30} of 152.5° C (see Figure 33). A 50/50 (by volume) mixture of the dissociation catalyst with AL-3996R (T_{30} = 148.5° C) exhibited a T_{30} of 150° C (see Figure 34). Although the product gas analyzer could not detect CO and H_2, the two catalysts appear to be compatible in that the effective activity of the 50/50 mixture as measured by T_{30} lies between the T_{30}'s of the two pure catalyst beds. Hence, no inhibition was measured.

Such a mixture makes a multi-reaction system possible

$$2CH_3OH \rightarrow CH_3OCH_3 + H_2O \rightarrow \text{higher hydrocarbons} \qquad (12)$$
$$\searrow \quad \swarrow$$
$$CO,\ H_2$$

Note that conversion of DME to CO and H_2 is also indicated. Tests analogous to the methanol dehydration but using DME demonstrated that the conversion of DME (presumably via dissociation) was equally feasible (Figure 35).

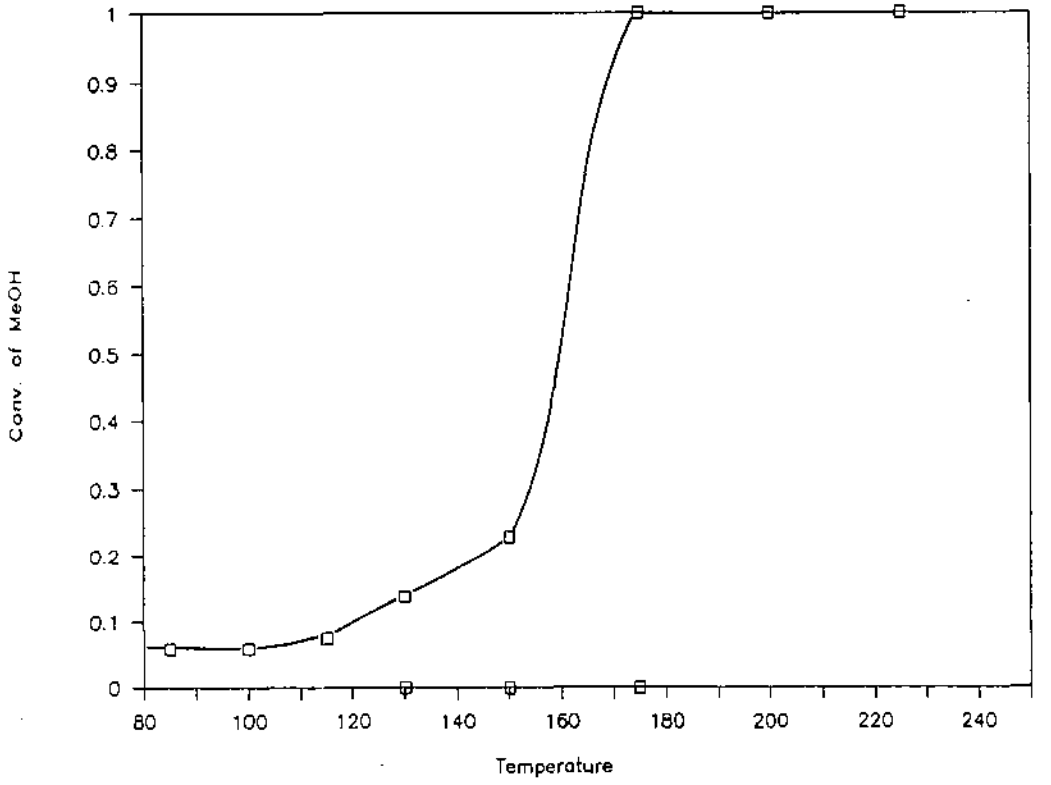

Figure 33. MeOH conversion, dissociation catalyst.

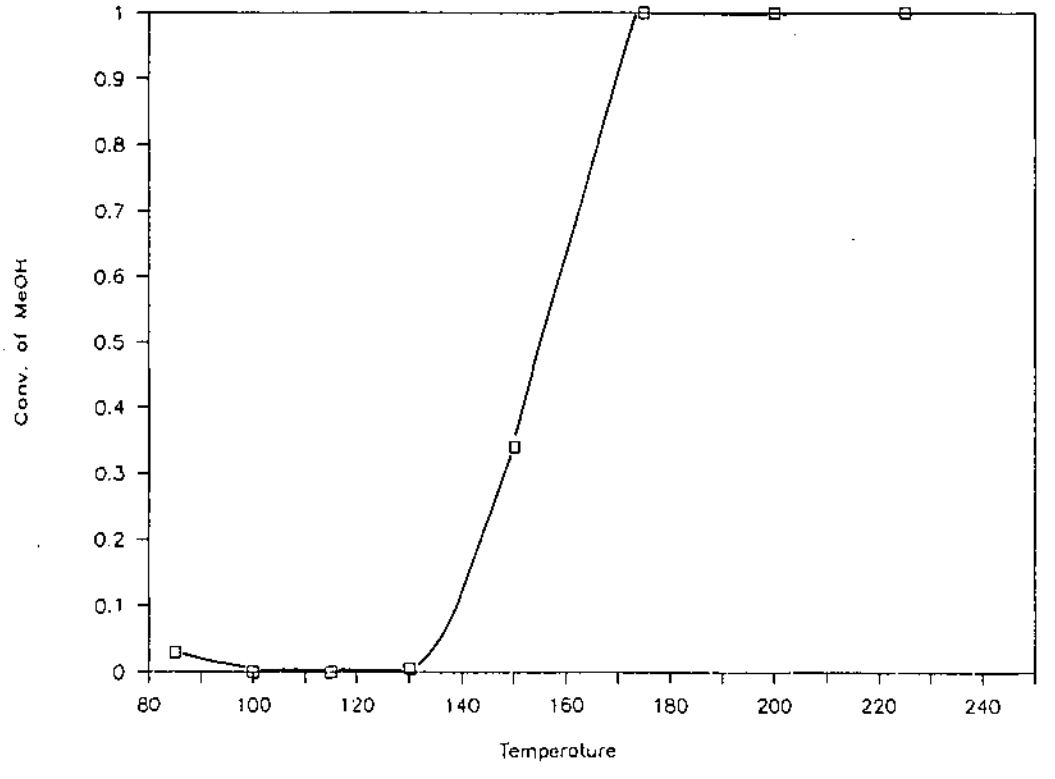

Figure 34. MeOH conversion, dissociation and AL 3996R.

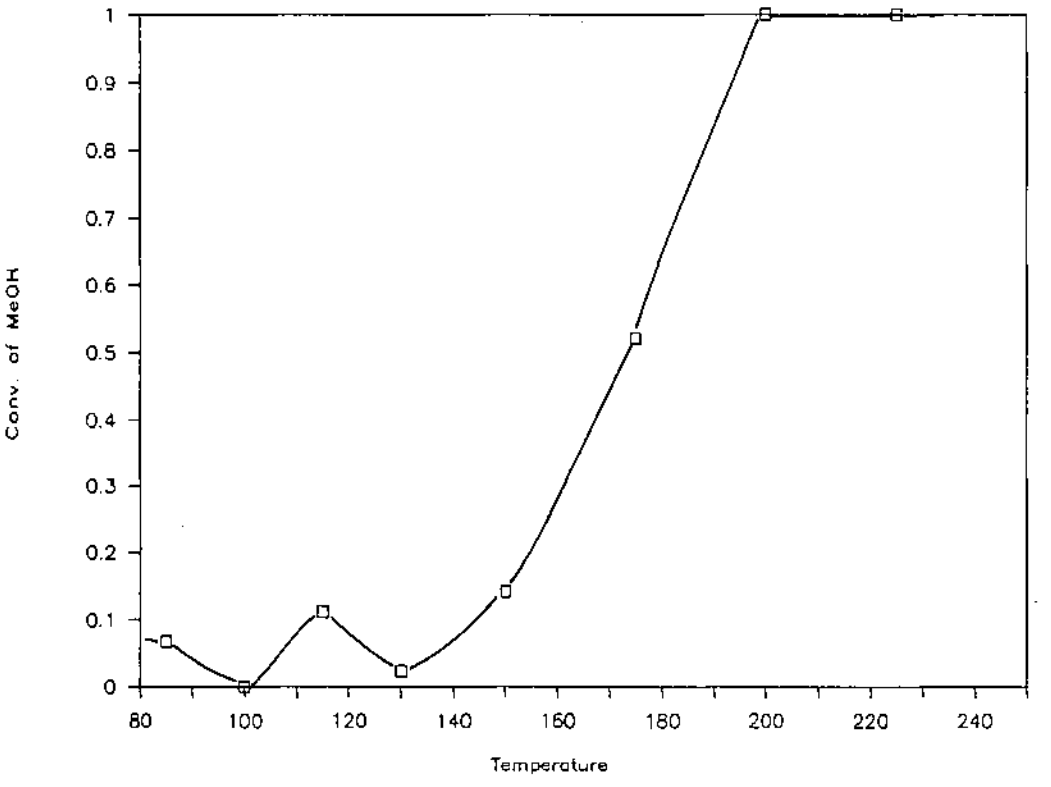

Figure 35. MeOH conversion, dissociation in DME.

The advantage of providing both dehydration and dissociation reaction pathways lies in relative heating requirements. The dissociation reaction requires approximately 20 kcal/mol of methanol consumed while methanol dehydration releases 2.2 kcal/mol. If a dehydration catalyst considerably more active than the dissociation catalyst was mixed with the dissociation catalyst, an *in-situ* safety net would be provided. As the dehydration reaction rate increased due to the liberation of heat, the dissociation reaction rate would begin to utilize more heat in the formation of CO and H_2.

A situation would exist which is analogous to the so-called predator (wolf) - prey (rabbit) system. In this scenario, the rabbit population is kept in check by an ever-present wolf population. In times of large rabbit proliferation (rapid dehydration rate) the wolf (dissociation rate) population grows due to the growing food supply. In turn, the wolf population is held in balance because the rabbit supply is consumed at a greater rate.

The selection of the appropriate dehydration catalyst (the wolf's food supply) will depend upon the relative effect of flow rate, heat transfer and both dehydration and dissociation reaction kinetics. To design and construct the

optimum reactor utilizing a dehydration/dissociation reaction system would require both the measurement of dehydration and dissociation kinetics and a reactor analysis based on the predator-prey model. Many of the latter theoretical descriptions exist in the applied mathematics literature so that no new modeling development is required. These models provide a steady state analysis which would be extremely useful in determining relative catalyst mixtures.

Process Energetics

Regardless of whether a pure DME catalyst or a mixture of methanol dehydration and dissociation catalyst are considered, an ultimate application of this contract is to design a prototype reactor system capable of starting a cold engine. If the liquid methanol fuel is initially at a very low temperature (say -10° C), the cold start apparatus must vaporize this liquid methanol and preheat it to the initial inlet condition needed for the dehydration reaction (approximately 200° C). Once in the reactor, the parameter sensitivity described in the previous section can be important due to the exothermicity of the dehydration reaction. It may be beneficial in this regard to add some dissociation catalyst. In any event, the heat given off by complete conversion of methanol to DME is given by:

$$\text{Heat given off by dehydration} = \frac{89.8\ \text{cm}^3}{\text{min}} \frac{0.7914\ \text{g}}{\text{cm}^3} \frac{\text{mol}}{32\text{g}} \frac{2.2 \times 10^3\ \text{kcal}}{\text{mol}} \quad (13)$$

$$= 4.9 \times 10^3\ \frac{\text{cal}}{\text{min}}.$$

The amount of heat required to bring the initially cold methanol to the inlet condition of the reactor (200° C) is given by

$$\text{Total heat}\ \left[\frac{\text{cal}}{\text{min}}\right] = \text{heat needed to raise liquid methanol to} + \text{heat of vaporization methanol to} + \text{heat needed to raise gaseous reactor condition} = 25 \times 10^3\ \left[\frac{\text{cal}}{\text{min}}\right] \quad (14)$$

Obviously, considerably more warm-up heat is consumed than is released by the dehydration reaction, even at a 100% conversion. Consequently, some additional heat must be made available before this apparatus can be used efficiently. This energy could conceivably be provided by the battery of the vehicle although given this energy availability it could be argued that the dehydration reactor itself is superfluous. That is, if the battery can provide 20×10^3 cal/min, it could certainly provide the additional 4.9×10^3 cal/min, thereby delivering a

stream of vaporized methanol at 200° C to the engine. Even so, this is unlikely to be feasible; an alternative process should be considered. This process is shown schematically as :

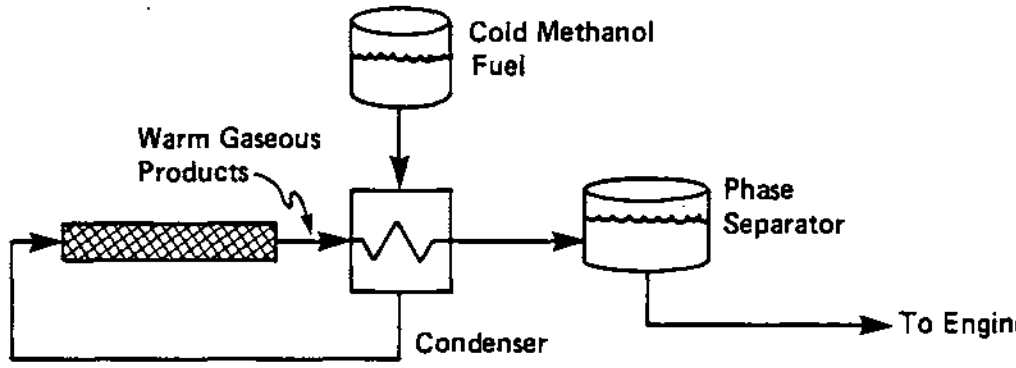

In this system the reactor products are assumed to be vapors at 200° C consisting of unconverted methanol, water, DME and perhaps a mixture of CO and hydrogen. The reactor exchanges heat with the incoming methanol feed stream, preheating it. The products are then passed through a condenser which liberates a significant amount of heat forming now a two-phase mixture. The vapor phase of this stream would consist of CO, H_2, some DME, water and methanol. The liquid stream would consist of liquid methanol, some water and DME. The proportions of DME in the vapor and liquid phases are dictated by the vapor-liquid phase equilibrium. A simple vapor-liquid equilibrium calculation is provided in Appendix E for the two component system of DME and methanol. The results show a liquid stream between 10 - 30° C should contain a DME mole fraction of roughly 10-20% DME. Since this mixture would exist under its own vapor pressure in the product phase separator, the liquid stream could be then pumped to the fuel system (i.e., fuel injectors). Once the mixture was sprayed in the cylinders or in the air intake, the DME would readily vaporize producing a combustible mixture suitable for starting the engine. This is very similar to the concept of winterized gasoline in which the lighter component of the gasoline is increased during the winter months.

SECTION 7
REFERENCES

1. Chang, C.D., and A.J. Silvestri, *J. Catal.*, 47:249-259, 1977.

2. Personal communication between RTI and Mobil Research and Development Co., 1988

3. Panzar, J., "Characteristics of Primed Methanol Fuels for Passenger Cars," SAE paper 831687.

4. Winterbottom, J.M., "Hydration and Dehydration by Heterogeneous Catalysts," in Catalysis-Specialist Periodical Report, Vol. 4, *Royal Society of Chemistry*, London, 141-174, 1981.

5. Swabb, E.A., and B.C. Gates, *Ind. Eng. Chem. Fund.*, 11(4), 1972.

6. Levenspiel, O. "Chemical Reaction Engineering," 2nd ed., Wiley, 1972.

7. Kramers, H., and K.R. Westerterp, *Elements of Chemical Reactor Design and Operation*, Academic Press, 1963.

8. Froment, G.F., and K.B. Bischoff, *Chemical Reactor Analysis and Design*, Wiley, 1979.

9. Bilous, O., and N.R. Amundson, AIChE Journal, *2*, 117, (1956).

10. Barkelew, C.H., Chem. Eng. Prog. Symp. Series No. 25, *55*, p. 37 (1959).

SECTION 8
SUMMARY AND FUTURE WORK

The research done in Phase I of this contract shows that there are commercial catalysts potentially suitable for the methanol dehydration reaction. This is evidenced by the wide range of dehydration activities as measured by T_{30} given in Table 2. Some problems exist, however, in the development of a prototype dehydration reactor. These were discussed in the Phase 2 plan of work. Primarily, the exothermicity of the methanol dehydration reaction can result in a runaway temperature excursion within the reactor. This can lead to loss of product selectivity by the formation of higher hydrocarbons with the concomitant formation of coke (carbonaceous material) which can lead to catalyst deactivation. Although more sophisticated reactor designs can be used to minimize the likelihood of these excursions, the reaction system is quite sensitive to slight changes in operating conditions. It is proposed to study the kinetic rates of both the methanol dehydration reaction over a limited group of candidate catalysts as well as the methanol dissociation reaction over the dissociation catalyst explored in Phase I. With this information, a relatively simple theoretical analysis is feasible by which a dehydration/dissociation mixture reactor could be designed. The dissociation reaction pathway would be provided only as a heat sink to prevent reactor runaway. Finally, it was noted that the process energetics would require the condensation of the product stream in order to allow operation without a significant amount of external power requirements. The condensed product stream is believed to be suitable for cold starting an internal combustion engine in a mechanism completely analogous to winterized gasoline.

It is recommended that the design parameters of a methanol dehydration/dissociation reactor be pursued to enable the design of a stable cold start apparatus. To that end the following work is proposed:

- study the reaction kinetics of the methanol dehydration over a select number of candidate catalysts
- study the reaction kinetics of the dissociation reaction over the dissociation catalyst explored in Phase I
- complete the reactor analysis required for optimal reactor designs and catalyst mixture proportions

- complete a more rigorous thermodynamic calculation of the multi-phase equilibrium formed by water, DME and methanol

It should be noted that the measurement of the chemical kinetic rates is a relatively simple task for which the equipment used for Phase 1 can be used with only slight modification (to include CO and hydrogen detection).

Although it is perhaps possible to design a prototype based exclusively on the methanol dehydration reaction using the data made available through Phase I, it is felt that the level of sophistication needed to control that reaction would be high making the expense of the ultimate reactor prohibitively large. Alternately, the dehydration/dissociation concept appears to be inherently stable, permitting a simpler design.

APPENDIX A
SOLICITATION FOR COMMERCIAL METHANOL DEHYDRATION CATALYSTS

Dear

Research Triangle Institute is involved with the developement of a system for the dehydration of methanol vapor to a mixture of dimethanol ether in water. The purpose of this research is to overcome cold start problems in methanol powered vehicles. The ultimate application of the catalyst and system which we will develop will be for such vehicles. Our immediate goal is twofold:

- Screening of a number of catalysts that are suitable for the dehydration of methanol to dimethanol ether.
- The assembly of a system using the best catalyst from our screening test to be tested on a stationary methanol powered automobile.

Our review of the literature on this reaction indicates that the dehydration of methanol is an intermediate step over acid catalyst with the ultimate products being light olefins and hydrocarbons. However, in contrast to processes such as the methanol to gasoline process, we wish to develop a catalyst that will produce dimethanol ether selectively. The literature also seemed to indicate that desirable catalyst characteristics are strong lewis acidity, little or no bromstead acidity, and weak lewis basicity. Conditions of interest for our study are atmospheric pressure, temperatures below about 350°C, and high space velocities.

We would appreciate your recommendations for catalyst that you may produce which could meet the objectives of our program. Specifically, we would appreciate your providing us with roughly 100 grams of candidate catalyst that you feel would work. In return, we will keep you advised of the results of our screening tests.

We plan to begin our screening in mid-December and would appreciate your providing samples for our use by then, if possible. We greatly appreciate your cooperation in this effort.

Please contact me at (919) 541-7272 to discuss any details of our goals and how your catalyst might be evaluated.

Sincerely,

James J. Spivey, Ph.D.

APPENDIX B
CALCULATION OF ADIABATIC TEMPERATURE RISE IN A TUBULAR REACTOR

The maximum temperature reached in a tubular reactor occurs when the reactants are completely converted under adiabatic conditions. This temperature known as the adiabatic temperature (T_{ad}) can be calculated using a standard expression as given by Kramers and Westerterp [1].

$$C_p \int_{T_o}^{T_{ad}} dT = \Delta H_r \int_{o}^{\xi_f} d\xi \qquad (B.1)$$

where C_p is the specific heat capacity of the gas stream, T_o is the temperature of the incoming stream, x is the molar fraction of the reacting species, ΔH_r is the heat of reaction and ξ is the fractional conversion. The maximum T_{ad} occurs when $\xi_f = 1$ (100% conversion). Although the equilibrium conversion of methanol to DME alone is limited to 85%, the DME can react further for higher hydrocarbons. This will allow complete depletion of the methanol.

Equation (B.1) can now be evaluated to yield

$$T_{ad} - T_o = -x \frac{\Delta H_r}{C_p} \xi_f \qquad (B.2)$$

For pure methanol forming DME (the heat of reaction due to the further reaction of DME is also exothermic but will be neglected),

$$\xi_f = 1$$

$$x = 1$$

$$\Delta H_r = -2.2 \times 10^3 \frac{cal}{mol}$$

$$C_p = 12.4 \frac{cal}{mol\ C}$$

$$T_o = 200°\ C \text{ (assumed inlet temperature)}$$

T_{ad} is calculated to be 377° C. If a feedstream of 1,000 ppm of methanol in nitrogen is converted,

$$x = 1 \times 10^{-3}$$

which yields a $T_{ad} - T_o$ of 0.18° C.

Reference

1. Kramers, H., and K.R. Westerterp, *Elements of Chemical Reactor Design and Operation*, Academic Press, 1963.

APPENDIX C
CALCULATION OF METHANOL REQUIRED TO START AN ENGINE

For the preliminary design of a prototype catalytic dehydrator, an estimate of the required methanol throughput is needed. To this end, the combustion energy required to start a spark ignition engine was assumed to be 6 kcal/sec (EPA). To satisfy cold starting requirements a product stream of 15% DME is needed [1] which corresponds to 30% conversion of methanol. To provide 6 kcal/sec assuming 15 mole % DME, the volumetric flow rate of gas from the dehydrator can be found as follows:

$$Q = \frac{6 \text{ kcal/sec}}{\Sigma\, x_i\, (-\Delta H_{ci})} \quad \frac{22{,}400 \text{ cm}^3}{\text{mol}}$$

where

Q = volumetric flowrate of gas from the dehydrator, cm^3/sec

x_i = mole fraction of component i, dimensionless

ΔH_{ci} = heat of combustion of component i, calculated herein at 25°C with all reactants and products as gases, kcal/mol

For our system

$$\Delta H_c\,(CH_3OH) = -160.3 \text{ kcal/mol}$$

$$\Delta H_c\,(CH_3OCH_3) = -331 \text{ kcal/mol}$$

$$\Delta H_c\,(H_2O) = 0 \text{ kcal/mol}$$

Substituting

$$Q = 829 \text{ cm}^3 \text{ STP/sec}$$

To result in 829 cm^3 STP/sec of gas containing 15% DME, 15% H_2O, and 70% methanol, the volume of liquid methanol, Q_m, that must be fed to the dehydrator is thus:

$$Q_m = 829 \frac{\text{cm}^3}{\text{sec}} \quad \frac{\text{mol gas}}{22{,}400 \text{ cm}^3 \text{ STP}} \quad \frac{\text{cm}^3 \text{ (liquid)}}{0.7914 \text{ g}} \quad \frac{32 \text{ g}}{\text{mol}} \quad \frac{60 \text{ min}}{\text{min}}$$

$$Q_m = 89.8 \frac{\text{cm}^3}{\text{min}} \text{ liquid methanol}$$

Reference

1. Panzar, J., "Characteristics of Primed Methanol Fuels for Passenger Cars," SAE paper 831687.

APPENDIX D
ESTIMATION OF GLOBAL KINETICS OF METHANOL DEHYDRATION

It is possible to use data presented in Section 3 to estimate the overall chemical kinetics of the methanol dehydration reaction,

$$2CH_3OH \rightleftharpoons CH_3OCH_3 + H_2O \qquad (D.1)$$

at an approximation for use in preliminary design. At low conversions (< 50%) reaction D.1 is far from equilibrium (see Section 2) so that only the forward reaction should be considered. For heterogeneous reaction systems a first order expression based on the volume of catalyst (m^3cat) can be assumed to approximate this reaction's rate,

$$r = k_v C \qquad (D.2)$$

where r is the rate of methanol conversion (m^3/hr m^3cat), k_v is the rate constant (m^3/hr m^3cat) and C is the concentration of methanol (M) in the feed (fd) (m^3M/m^3fd).

In estimating the rate constant from data measured in the tubular microreactor, an analysis similar to that given by Kramers and Westerterp [1, p. 25] will be used. That analysis shows that, at steady state, the extent of conversion, ξ, of a reactant varies with distance along the axis of the reactor, z, according to,

$$\frac{d\xi}{dz} = \frac{r\, S_{cat}}{\phi_v} \qquad (D.3)$$

where S_{cat} is the cross-sectional area of catalyst and ϕ_v is the volumetric flowrate of methanol (m^3 hr) fed to the reactor at reactor conditions. This expression can be rearranged and integrated to give

$$\int_0^{\xi_f} \frac{\phi_v}{r}\, d\xi = \int_0^{V_{cat}} S_{cat}\, dz \qquad (D.4)$$

where ξ_f is the extent of conversion at the reactor outlet and V_{cat} is the total volume of catalyst in the reactor. According to reaction (D.1) the gas mixture's density should remain constant. The rate expression (D.2) can be rewritten in terms of the extent of reaction as.

$$r = k_v C_o (1-\xi) \tag{D.5}$$

where C_o is the concentration of methanol in the feedstream at the reactor inlet. Equation E.1 can now be integrated to yield,

$$\frac{-\phi_v}{k_v C_o} \ln(1 - \xi_f) = V_{cat} \tag{D.6}$$

This expression can be solved for k_v,

$$k_v = - \frac{\phi_v}{C_o V_{cat}} \ln(1 - \xi_f) \tag{D.7}$$

For the catalyst screening tests described in Section 3 the following values apply

$$\phi_v = 1.2 \times 10^{-5}\ m_M^3/hr$$

$$C_o = 1.0 \times 10^{-3}\ m_M^3/m^3fd$$

$V_{cat} = (1 - \epsilon)V_r = (1 - 0.3)(5.03 \times 10^{-7}\ m^3) = 3.52 \times 10^{-7} m^3cat$.

Here V_r is the total reactor volume (4 mm I.D., 40 mm long) and ϵ is the approximate void fraction in the reactor.

In this manner the first order rate constant can be calculated for any catalyst tested under Phase I. For the purpose of the preliminary design work presented here, the results of catalyst AL-5207 (Harshaw) presented in Figure 28 will be used:

$$k_v = - \frac{(1.2 \times 10^{-5}(m_M^3/hr)}{(1.0 \times 10^{-3}(m_M^3/m^3fd)(3.52 \times 10^{-7} m^3cat)} \ln(1-0.25) \tag{D.8}$$

The rate constant is a function of reactor temperature

$$k_v = Ae^{-E/RT} \tag{D.9}$$

where A is the pre-exponential factor, E is the activation energy of the reaction on the particular catalyst, R is the gas constant and T the temperature in Kelvin. The activation energy can be estimated by plotting the ln k vs 1/T for a number of reactor temperatures, as follows:

T (°C)	ξ	k	ln k	1/T (K^{-1})
126	0.1	3.6×10^3	8.2	2.51×10^{-3}
134	0.2	7.6×10^3	8.9	2.46×10^{-3}
136.5	0.25	9.8×10^3	9.2	2.44×10^{-3}
139.5	0.3	1.2×10^4	9.4	2.42×10^{-3}

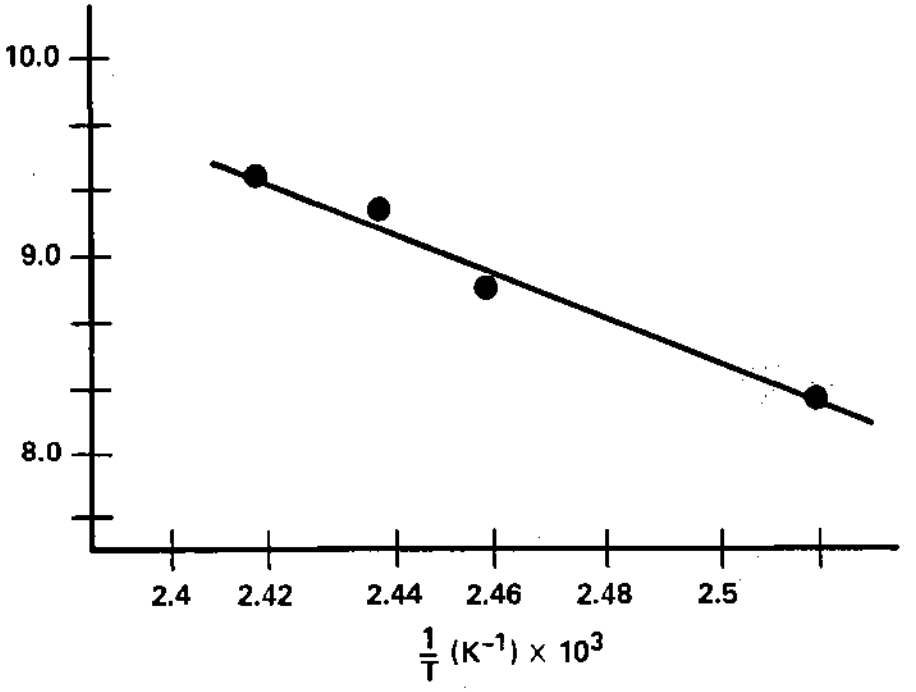

The slope of this curve is, then, $E/R = 13.6 \times 10^3$ K. The apparent activation energy E, of this reaction on AL-5207 is approximately 27 kcal/mol.

Reference

1. Kramers, H., and K.R. Westerterp, *Elements of Chemical Reactor Design and Operation*, Academic Press, 1963.

APPENDIX E
CALCULATION OF THE VAPOR-LIQUID EQUILIBRIUM (VLE) DATA FOR A TWO-COMPONENT MIXTURE OF DME AND METHANOL*

A first approximation to the vapor-liquid equilibrium relationship for a binary mixture of dimethyl-ether (DME) in methanol (MeOH) at 1 atm pressure is given by:

$$\text{For DME,} \quad Y_{DME} = K_{DME} X_{DME} \tag{E.1}$$

where y is the vapor-phase mole fraction, K is the proportionality constant to be determined, and X is the liquid phase mole fraction.

$$\text{For MeOH,} \quad Y_{MeOH} = K_{MeOH} X_{MeOH} \tag{E.2}$$

The addition of (E.1) and (E.2) yields

$$X_{DME} = \frac{(1 - K_{MeOH})}{(K_{DME} - K_{MeOH})} .$$

Two methods will be used:

Method 1: Assume Henry's Law for K_{DME}
Assume Raoult's law for K_{MeOH}

$$K_{DME} = \gamma^{\infty}_{DME} P^{sat}_{DME}$$

$$K_{MeOH} = P^{sat}_{MeOH}$$

The infinite dilution activity coefficient for DME, γ^{∞}_{DME}, was calculated using UNIFAC (Universal Quasi Chemical Functional-Group Activity Coefficient model) while P^{sat}, the vapor pressure of both components, was calculated by Antoine's equation.

The VLE results are given in Table E-1 for both 10° C and 30° C.

*Source: Tony Rogers, RTI.

Table E-1

Temperature (°C)	$\gamma^{\infty}_{D}M$	P^{sat}_{DME}	X_{DME}(%)
10	1.47	3.81	16.8
30	1.5	7.08	7.6

Method 2: Assume Raoult's law for both DME and MeOH

$$K_{DME} = P^{sat}_{MeOH}$$

$$K_{MeOH} = P^{sat}_{MeOH}$$

The VLE results are given in Table E-2 for both 10° C and 30° C.

Table E-2

Temperature (°C)	P^{sat}_{DME}	X_{DME}(%)
10	3.81	24.7
30	7.08	11.5

The actual liquid-phase DME concentration will likely be between the extremes shown in the above tables. Because the target reactor conversion of methanol is roughly 30%, the DME concentration at the phase separator will be approximately 15%. This is substantially above infinite dilution of DME in methanol, so the Raoult's law results are thought to be more accurate. Note, however, that the proportionality constant, K, is concentration dependent and a more involved iterative procedure should be used to predict X_{DME} with greater accuracy.